HIGH TEMPERATURE CHEMISTRY OF SOME BOROPHOSPHATES, PHASE RELATIONS AND STRUCTURAL STUDIES

A THESIS SUBMITTED TO
THE GRADUATE SCHOOL OF NATURAL AND APPLIED SCIENCES
OF THE MIDDLE EAST TECHNICAL UNIVERSITY

BY

SEMİH SEYYİDOĞLU

IN PARTIAL FULFILLMENT OF THE REQUIREMENTS FOR THE DEGREE OF
MASTER OF SCIENCE
IN
THE DEPARTMENT OF CHEMISTRY

AUGUST 2003

Approval of Graduate School of Natural and Applied Sciences

_____

Prof.Dr. Canan Özgen
Director

I certify this thesis satisfies all the requirements as a thesis for the degree of Master of Science

_____

Prof.Dr. Teoman Tinçer
Head of the Department

This is to certify that we have read this thesis and that in our opinion it is fully adequate, in scope and quality, as a thesis for the degree of Master of Science.

_____

Prof.Dr. Meral Kızılyallı
Supervisor

Examining Committee Members:

Prof.Dr. Meral Kızılyallı _____

Prof.Dr. Şahinde Demirci _____

Assoc.Prof.Dr. Ceyhan Kayran _____

Prof.Dr. Gülhan Özbayoğlu _____

Prof.Dr. Yavuz Topkaya _____

ABSTRACT

HIGH TEMPERATURE CHEMISTRY OF SOME BOROPHOSPHATES, PHASE RELATIONS AND STRUCTURAL STUDIES

Seyyidoğlu, Semih

M.Sc. Thesis, Department of Chemistry
Supervisor: Prof. Dr. Meral Kızılyallı

August 2003, 94 pages

The solid state, hydrothermal and flux methods were used for the investigation of alkaline earth and transition metal borophosphate compounds. The products and the phase relations were investigated by XRD, IR, DTA, and EDX methods. The solid state reactions of several boron compounds with different phosphating agents have been studied in the temperature range of 400-1200 ^{o}C. Hydrothermal and flux techniques were performed at 150 ^{o}C and 1200 ^{o}C, respectively.

On the other hand, an attempt has been made to prepare a novel borophosphate compound $M^{II}M^{IV}[BPO_7]$ (where $M^{IV}= Zr^{4+}$, Si^{4+}, and $M^{II}= Sr^{2+}$, Ca^{2+}) by solid state reactions and to investigate intermediate and final products. $(NH_4)_2HPO_4$ and $NH_4H_2PO_4$ were used as a phosphating agent. For the synthesis of these new compounds, the following reaction was predicted using the stoichiometric amount of the reactants:

$2M^{IV}O_2 + 2M^{II}CO_3 + B_2O_3 + 2(NH_4)_2HPO_4 \rightarrow 2M^{II}O.M^{IV}O_2.B_2O_3.P_2O_5 + 4NH_3 + 3H_2O + 2CO_2$ (According to IUPAC formulation for the compounds composed of oxides)

In the case of $M^{IV}=Zr^{4+}$ and $M^{II}=Sr^{2+}$, the formation of $ZrSr[BPO_7]$ was observed together with ZrO_2 and $SrBPO_5$. The formation of a new phase was proved

by indexing the XRD pattern of the product after separating ZrO_2 and $SrBPO_5$ lines. Its crystal system was found to be orthorhombic and the unit cell parameters are a=11.85Å, b=12.99 Å, c=17.32 Å. IR analysis shows that there is $[BPO_7]^{6-}$ bands in the spectrum. At higher temperatures, $Sr_7Zr(PO_4)_6$ was obtained. In the case of $M^{IV}=Si^{4+}$, $SrBPO_5$ was the main product together with unreacted SiO_2. At 1100 ^oC, Si^{4+} entered $SrBPO_5$ structure and the product was indexed in orthorhombic system with a=8.9243 Å, b=13.1548 Å, and c=5.4036 Å.

Several other M:B:P ratios were tried for solid state systems. For compositions with different cations (such as Al^{3+}, Ca^{2+}, Na^{+}), reactions generally pass through metal phosphates and BPO_4.

The X-ray diffraction powder pattern and infrared spectrum of several intermediate products obtained at different temperatures were presented and the several phase relations were investigated. The DTA and EDX analyses of some products were also reported.

Keywords: Borophosphate compounds, phase relations in borophosphates, alkaline earth and transition metal borophosphates, IR, X-ray powder diffraction, solid-state, hydrothermal, flux methods, EDX.

ÖZ

BAZI YENİ BOROFOSFAT BİLEŞİKLERİNİN YÜKSEK SICAKLIK KİMYASI, FAZ BAĞINTILARI VE YAPI ÇALIŞMALARI

Seyyidoğlu, Semih

Yüksek Lisans Tezi, Kimya Bölümü
Tez Yöneticisi: Prof. Dr. Meral Kızılyallı

Ağustos 2003, 94 sayfa

Toprak alkali ve geçiş metallerinin borofosfat bileşiklerinin araştırılmasında katı hal, eritiş ve hidrotermal yöntemleri kullanılmıştır. Elde edilen ürünler XRD, IR, DTA ve EDX yöntemleri ile incelenmiştir. Çeşitli borlu bileşiklerin farklı fosfatlayıcı bileşiklerle olan katı hal tepkimeleri 400-1200 ^{o}C sıcaklık aralığında çalışılmıştır. Hidrotermal ve eritiş yöntemleri sırasıyla 150 ^{o}C ve 1200 ^{o}C sıcaklıklarında çalışılmıştır.

Diğer taraftan $M^{II}M^{IV}[BPO_7]$ (M^{IV}= Zr^{4+}, Si^{4+} ve M^{II}= Sr^{2+}, Ca^{2+}) türündeki yeni borofosfat bileşiklerini katı hal yöntemiyle hazırlamak, ara ve son ürünleri XRD ve IR çalışmalarıyla incelemek için bazı tepkimeler denenmiştir. Tepkimelerde genel olarak, $(NH_4)_2HPO_4$ ve $NH_4H_2PO_4$ fosfatlayıcı bileşikler olarak kullanılmıştır. Bu yeni uç ürünlerin üretiminde aşağıdaki denklemde oranları belirtilen bir tepkime öngörülmüştür:

$2M^{I}O_2 + 2M^{II}CO_3 + B_2O_3 + 2(NH_4)_2HPO_4 \rightarrow 2M^{II}O.M^{IV}\ O_2.B_2O_3.P_2O_5 + 4NH_3 + 3H_2O + 2CO_2$ (IUPAC Kurallarına göre bileşik oksitlerden oluşan şekliyle verilmiştir)

M^{IV}=Zr^{4+} ve M^{II}=Sr^{2+} durumunda $ZrSr[BPO_7]$ bileşiğinin, ZrO_2 ve $SrBPO_5$ bileşikleri ile birlikte elde edildiği görülmüştür. Bu yeni bileşiğin oluşumu, XRD izlerinden tepkimeye katılmayan bir kısım ZrO_2 ve yeni oluşan $SrBPO_5$ kırınımları

ayrıldıktan sonra, kalan izlerin indekslenmesi ile ispatlanmıştır. Kristal sistemi a=11,85Å, b=12,99 Å, c=17,32 Å birim hücre boyutları ile ortorombik sistemde indekslenmiştir. Sistemin IR spektroskopisi yöntemiyle incelenmesi sonucu, $[BPO_7]^{6-}$ anyonu içeren pikler görülmüştür. Yüksek sıcaklıklarda ise, genellikle $Sr_7Zr(PO_4)_6$ bileşiğinin yan ürün olarak oluştuğu bulunmuştur. $M^{IV}=Si^{4+}$ kullanıldığında $SrBPO_5$, tepkimeye girmeyen SiO_2 ile birlikte elde edilmiş ve 1100 ^oC'de, Si^{4+} $SrBPO_5$ yapısına girdiği anlaşılmıştır. Oluşan bileşik a=8,9243 Å, b=13,1548 Å ve c=5,4036 Å birim hücre boyutlarıyla ortorombik sistemde indekslenmiştir.

Bir çok M:B:P oranı çeşitli katı hal sistemlerinde denenmiştir. Değişik katyonlu (örneğin Al^{3+}, Ca^{2+}, Na^{+}) tepkimelerin genellikle metal fosfat ve BPO_4 üzerinden geçtiği ispatlanmıştır.

Değişik sıcaklıklarda elde edilen ürünlerin X-ışınları kırınım izleri ve kızılötesi spektrumu verilerek faz bağıntıları incelenmiştir. Bazı ürünlerin DTA ve EDX ölçümleri de verilmiştir.

Anahtar Kelimeler: Borofosfat bileşikleri, borofosfat bileşiklerinin faz bağıntıları, toprak alkali ve geçiş metal borofosfat bileşikleri, IR, X-ışınları toz kırınımı, katı-hal, hidrotermal, eritiş yöntemleri, EDX.

To my brother Emin Ferhan, my father Ömer Faruk,
my mother Fatma Bengi Seyyidoğlu, and
to my supervisor Meral Kızılyallı

ACKNOWLEDGEMENTS

I would like to express my graditude to Prof.Dr. Meral Kızılyallı for her guidance, continious encouragement, critical discussion and patience at every stage of this thesis.

I am most grateful to Department of Chemistry of M.E.T.U for supplying every kind of necessities during my study.

I am grateful to my family for their support by all means, especially to my mother Bengi Seyyidoğlu.

I wish to extend my sincere thanks to Özkan Şengül for his continious help in German and computer work, Chemistry Society of M.E.T.U for their help, Seriya Genceliova who opened a way to read Russian Chemistry Journals,Yusuf Güner for his help in IR analysis, Senem Kıralp for her help at the final stage of this thesis, and Ceren Obakan for her patience.

Finally, I also would like to thank Graduate School of Natural Applied Sciences for funding my thesis with the project number of BAP-2002-07-02-00-90, and DPT Project No:BAP-01-03-DPT-2003K-120920-09.

TABLE OF CONTENTS

LIST OF TABLES

LIST OF FIGURES

ABSTRACT

HIGH TEMPERATURE CHEMISTRY OF SOME BOROPHOSPHATES, PHASE RELATIONS AND STRUCTURAL STUDIES

Seyyidoğlu, Semih

M.Sc. Thesis, Department of Chemistry
Supervisor: Prof. Dr. Meral Kızılyallı

August 2003, 94 pages

The solid state, hydrothermal and flux methods were used for the investigation of alkaline earth and transition metal borophosphate compounds. The products and the phase relations were investigated by XRD, IR, DTA, and EDX methods. The solid state reactions of several boron compounds with different phosphating agents have been studied in the temperature range of 400-1200 ^{o}C. Hydrothermal and flux techniques were performed at 150 ^{o}C and 1200 ^{o}C, respectively.

On the other hand, an attempt has been made to prepare a novel borophosphate compound $M^{II}M^{IV}[BPO_7]$ (where M^{IV}= Zr^{4+}, Si^{4+}, and M^{II}= Sr^{2+}, Ca^{2+}) by solid state reactions and to investigate intermediate and final products. $(NH_4)_2HPO_4$ and $NH_4H_2PO_4$ were used as a phosphating agent. For the synthesis of these new compounds, the following reaction was predicted using the stoichiometric amount of the reactants:

$2M^{IV}O_2 + 2M^{II}CO_3 + B_2O_3 + 2(NH_4)_2HPO_4 \rightarrow 2M^{II}O.M^{IV}O_2.B_2O_3.P_2O_5 + 4NH_3 + 3H_2O + 2CO_2$ (According to IUPAC formulation for the compounds composed of oxides)

In the case of $M^{IV}=Zr^{4+}$ and $M^{II}=Sr^{2+}$, the formation of $ZrSr[BPO_7]$ was observed together with ZrO_2 and $SrBPO_5$. The formation of a new phase was proved by indexing the XRD pattern of the product after separating ZrO_2 and $SrBPO_5$ lines. Its crystal system was found to be orthorhombic and the unit cell parameters are a=11.85Å, b=12.99 Å, c=17.32 Å. IR analysis shows that there is $[BPO_7]^{6-}$ bands in the spectrum. At higher temperatures, $Sr_7Zr(PO_4)_6$ was obtained. In the case of $M^{IV}=Si^{4+}$, $SrBPO_5$ was the main product together with unreacted SiO_2. At 1100 ^oC, Si^{4+} entered $SrBPO_5$ structure and the product was indexed in orthorhombic system with a=8.9243 Å, b=13.1548 Å, and c=5.4036 Å.

Several other M:B:P ratios were tried for solid state systems. For compositions with different cations (such as Al^{3+}, Ca^{2+}, Na^{+}), reactions generally pass through metal phosphates and BPO_4.

The X-ray diffraction powder pattern and infrared spectrum of several intermediate products obtained at different temperatures were presented and the several phase relations were investigated. The DTA and EDX analyses of some products were also reported.

Keywords: Borophosphate compounds, phase relations in borophosphates, alkaline earth and transition metal borophosphates, IR, X-ray powder diffraction, solid-state, hydrothermal, flux methods, EDX.

ÖZ

BAZI YENİ BOROFOSFAT BİLEŞİKLERİNİN YÜKSEK SICAKLIK KİMYASI, FAZ BAĞINTILARI VE YAPI ÇALIŞMALARI

Seyyidoğlu, Semih

Yüksek Lisans Tezi, Kimya Bölümü
Tez Yöneticisi: Prof. Dr. Meral Kızılyallı

Ağustos 2003, 94 sayfa

Toprak alkali ve geçiş metallerinin borofosfat bileşiklerinin araştırılmasında katı hal, eritiş ve hidrotermal yöntemleri kullanılmıştır. Elde edilen ürünler XRD, IR, DTA ve EDX yöntemleri ile incelenmiştir. Çeşitli borlu bileşiklerin farklı fosfatlayıcı bileşiklerle olan katı hal tepkimeleri 400-1200 ^{o}C sıcaklık aralığında çalışılmıştır. Hidrotermal ve eritiş yöntemleri sırasıyla 150 ^{o}C ve 1200 ^{o}C sıcaklıklarında çalışılmıştır.

Diğer taraftan $M^{II}M^{IV}[BPO_7]$ (M^{IV}= Zr^{4+}, Si^{4+} ve M^{II}= Sr^{2+}, Ca^{2+}) türündeki yeni borofosfat bileşiklerini katı hal yöntemiyle hazırlamak, ara ve son ürünleri XRD ve IR çalışmalarıyla incelemek için bazı tepkimeler denenmiştir. Tepkimelerde genel olarak, $(NH_4)_2HPO_4$ ve $NH_4H_2PO_4$ fosfatlayıcı bileşikler olarak kullanılmıştır. Bu yeni uç ürünlerin üretiminde aşağıdaki denklemde oranları belirtilen bir tepkime öngörülmüştür:

$2M^{I}O_2 + 2M^{II}CO_3 + B_2O_3 + 2(NH_4)_2HPO_4 \rightarrow 2M^{II}O.M^{IV}\ O_2.B_2O_3.P_2O_5 + 4NH_3 + 3H_2O + 2CO_2$ (IUPAC Kurallarına göre bileşik oksitlerden oluşan şekliyle verilmiştir)

$M^{IV}=Zr^{4+}$ ve $M^{II}=Sr^{2+}$ durumunda $ZrSr[BPO_7]$ bileşiğinin, ZrO_2 ve $SrBPO_5$ bileşikleri ile birlikte elde edildiği görülmüştür. Bu yeni bileşiğin oluşumu, XRD izlerinden tepkimeye katılmayan bir kısım ZrO_2 ve yeni oluşan $SrBPO_5$ kırınımları ayrıldıktan sonra, kalan izlerin indekslenmesi ile ispatlanmıştır. Kristal sistemi a=11,85Å, b=12,99 Å, c=17,32 Å birim hücre boyutları ile ortorombik sistemde indekslenmiştir. Sistemin IR spektroskopisi yöntemiyle incelenmesi sonucu, $[BPO_7]^{6-}$ anyonu içeren pikler görülmüştür. Yüksek sıcaklıklarda ise, genellikle $Sr_7Zr(PO_4)_6$ bileşiğinin yan ürün olarak oluştuğu bulunmuştur. $M^{IV}=Si^{4+}$ kullanıldığında $SrBPO_5$, tepkimeye girmeyen SiO_2 ile birlikte elde edilmiş ve 1100 ^oC'de, Si^{4+} $SrBPO_5$ yapısına girdiği anlaşılmıştır. Oluşan bileşik a=8,9243 Å, b=13,1548 Å ve c=5,4036 Å birim hücre boyutlarıyla ortorombik sistemde indekslenmiştir.

Bir çok M:B:P oranı çeşitli katı hal sistemlerinde denenmiştir. Değişik katyonlu (örneğin Al^{3+}, Ca^{2+}, Na^{+}) tepkimelerin genellikle metal fosfat ve BPO_4 üzerinden geçtiği ispatlanmıştır.

Değişik sıcaklıklarda elde edilen ürünlerin X-ışınları kırınım izleri ve kızılötesi spektrumu verilerek faz bağıntıları incelenmiştir. Bazı ürünlerin DTA ve EDX ölçümleri de verilmiştir.

Anahtar Kelimeler: Borofosfat bileşikleri, borofosfat bileşiklerinin faz bağıntıları, toprak alkali ve geçiş metal borofosfat bileşikleri, IR, X-ışınları toz kırınımı, katı-hal, hidrotermal, eritiş yöntemleri, EDX.

To my brother Emin Ferhan, my father Ömer Faruk,
my mother Fatma Bengi Seyyidoğlu, and
to my supervisor Meral Kızılyallı

ACKNOWLEDGEMENTS

I would like to express my graditude to Prof.Dr. Meral Kızılyallı for her guidance, continious encouragement, critical discussion and patience at every stage of this thesis.

I am most grateful to Department of Chemistry of M.E.T.U for supplying every kind of necessities during my study.

I am grateful to my family for their support by all means, especially to my mother Bengi Seyyidoğlu.

I wish to extend my sincere thanks to Özkan Şengül for his continious help in German and computer work, Chemistry Society of M.E.T.U for their help, Seriya Genceliova who opened a way to read Russian Chemistry Journals,Yusuf Güner for his help in IR analysis, Senem Kıralp for her help at the final stage of this thesis, and Ceren Obakan for her patience.

Finally, I also would like to thank Graduate School of Natural Applied Sciences for funding my thesis with the project number of BAP-2002-07-02-00-90, and DPT Project No:BAP-01-03-DPT-2003K-120920-09.

TABLE OF CONTENTS

LIST OF TABLES

LIST OF FIGURES

CHAPTER I

INTRODUCTION

1.1. Boron-Oxygen Chemistry

The element boron with the atomic number 5 has the electron configuration: $1s^2\ 2s^2\ 2p^1$ and is placed in Group 13 of the periodic classification. The elemental form of boron is unstable in nature. Boron is found combined with mainly oxygen in a wide variety of hydrated alkali and alkaline earth-borate salts and borosilicates.

The oxidation state of boron is 3+ and the element normally combines with oxygen to form three triangular-planar bonds by sp^2 orbital hybridization. The transition to tetrahedral sp^3 orbital hybridization state is facilitated by the easy acceptance of an electron-pair from a base into the low-energy fourth orbital of the boron valence shell. The measured B-O bond distances range from 1.28 Å to 1.44 Å and the mean is 1.37 Å in trigonal borates. The mean in tetrahedral borates is 1.48 Å and the individual values vary from 1.42 to 1.54 Å [1]. Table 1.1 gives B-O distances of some triangular and tetrahedral borates.

Boron may be considered as a typical metalloid having properties intermediate between the metals and the electronegative non-metals. The tendency for boron is to form anionic complexes rather than cationic ones. The formation of the hydroxyborate ion from a water solution of boric acid is given below.

$$B(OH)_3 + H_2O \leftrightarrow B(OH)_4^- + H^+$$

Table 1.1. B-O Bond Distances of Some Triangular and Tetrahedral Borates [1]

Compound	**B-O, Å Triangular BO_3**	**B-O, Å Tetrahedral BO_4**
Bandlyte $CuB(OH)_4Cl$	-	1.42
Boracite $Mg_7B_3O_{13}$	1.39	1.48
Borax $Na_2B_4O_5(OH)_4.8H_2O$	1.32, 1.36, 1.40	1.46, 1.47, 1.54
Boric Acid $B(OH)_3$	1.365, 1.356	-
Boron Phosphate BPO_4	-	1.44
Cesium Triborate CsB_3O_5	1.35, 1.39, 1.41, 1.34, 1.37, 1.44	1.45, 1.46, 1.49, 1.50
Colemanite $CaB_3O_4(OH)_3.H_2O$	1.36, 1.37, 1.39	1.44, 1.45, 1.47,1.49, 1.51, 1.52, 1.50
Hydrates of the above	1.38(av.)	1.48
Potassium metaborate KBO_2	1.33, 1.38	-
Potassium pentaborate dihydrate $KB_5O_6(OH)_4.2H_2O$	1.37, 1.39, 1.42, 1.28, 1.33, 1.34	1.53

Boron, like silicon, occurs in nature exclusively as oxy-compounds, especially hydroxyborates of calcium and sodium. BO_3 coordination group containing borates has a simple relation between the O:B ratio and the number of O atoms shared by each BO_3 group, assuming these to be equivalent and each bonded to 2B atoms as given in Table 1.2.

Table 1.2. O:B Ratio of Different Types of Borates [2]

O:B Ratio	Borate Types	Number of O Atoms Shared
3	Orthoborates:discrete BO_3^{3-} ions	0
2.5	Pyroborates:discrete $B_2O_5^{4-}$ ions	1
2	Metaborates:cyclic or chain ions	2
1.5	Boron trioxide	3

In 3-coordinated borates, all of the above four possibilities are realized, but there are two factors which complicate the oxygen chemistry of boron. First, there is tetrahedral coordination of B in many oxy-compounds. Second, there are many hydroxyborates containing OH bonded to B as part of a 3- or 4- coordination group; that is marked contrast to the rarity of hydroxysilicates. Examples of this situation are known of all 4-coordination groups from BO_4 through $BO_3(OH)$ and $BO_2(OH)_2$, both of which occur in $CaB_3O_4(OH)_3.H_2O$, and $BO(OH)_3$ (in $Mg[B_2O(OH)_6]$) to $B(OH)_4$ in tetrahydroxyborates such as $NaB(OH)_4$ [2].

1.1.1. Classification of B-O Compounds

1.1.1.1. Boron Trioxide, B_2O_3

Boron trioxide may be crystallized by dehydrating boric or metaboric acid under carefully controlled conditions [1-3] although it was known only in the vitreous state until as late as 1937. The structure of crystalline boric oxide as a system of spiral chains of interconnected tetrahedra similar to that of α-quartz; this consists of borate tetrahedra that were depicted as forming trimeric rings such as in quartz. Three of the oxygen corners of the tetrahedra are shared with two other tetrahedra, giving rise to tricoordinate oxygen, which is an unusual situation. The fourth oxygen atom is shared by only two tetrahedra as in quartz. In SiO_2 quartz-type, boric oxide would be oxygen deficient [4,5].

1.1.1.2. Orthoboric acid, and Orthoborates

The crystal structure of boric acid was refined by Zachariasen [6,7] using X-ray diffraction. It is composed of discrete $B(OH)_3$ molecules linked together by hydrogen bonds, O-H----O, to form infinite layers of approximately hexagonal symmetry given in Figure 1.1.

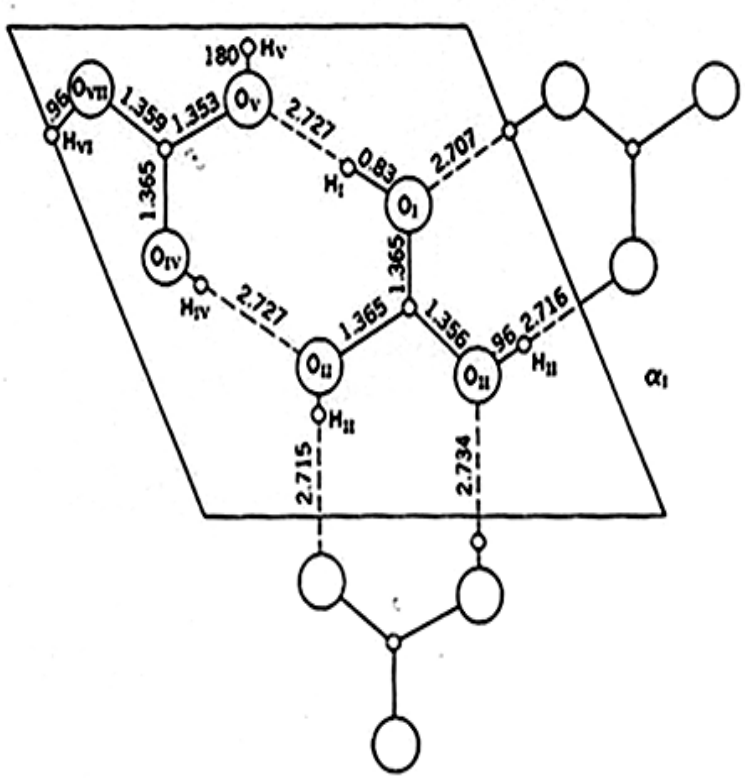

Figure 1.1. The Crystal Structure of H_3BO_3 [1]

1.1.1.3. Pyroborates (Diborates)

The pyroborate ion, $(B_2O_5)^{4-}$, given in Figure 1.2, consists of two triangles joined by a common oxygen and occurs in magnesium and cobalt salts [8,9].

1.1.1.4. Metaborates: Cyclic or Chain Ions

Metaboric acid is produced by dehydration of orthoboric acid below 130°C.

$$H_3BO_3 \rightarrow HBO_2 + H_2O$$

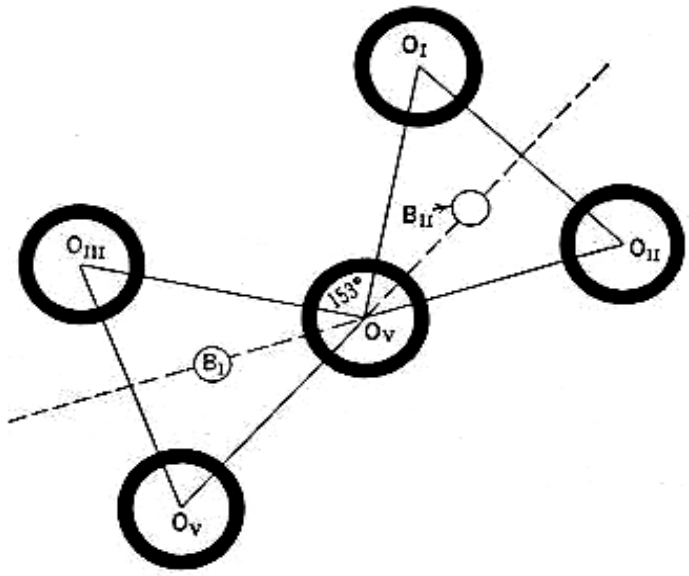

Figure 1.2 The Crystal Structure of Pyroborate [8,9]

In this case, the formation of orthorhombic metaboric acid is observed. The structure of HBO_2 consists of layers of trimeric B_3O_6 rings connected by hydrogen bonds [10]. Metaborates are anhydrous compounds with the formula of $M_x(BO_2)_y$; certain compounds originally formulated as hydrated metaborates contain $B(OH)_4^-$ ions; for example, $NaBO_2.4H_2O$ is $NaB(OH)_4.2H_2O$ [2].

1.1.1.5. Hydroxyborates

Another type of boron-oxygen compounds are hydroxyborates. In this group, the number of possible anions is large since:

a) there are different basic ring systems
b) the number of extra-annular oxygen atoms can in principle increase until all the B atoms are 4-coordinated
c) the extra-annular oxygen atoms can be O of OH atoms could be either unshared or shared between two units;
d) a particular borate anion may be built of units all of the same kind or it may be built from units of two or more kinds [2].

1.2. Boron-Deposits in Turkey

Turkey has the largest boron deposits in the world. In the case of B_2O_3, Turkey has 63% of the worlds total B_2O_3 deposits as given in Table 1.3 .

Table 1.3. Boron Reserves of Some Countries [11]

Countries	**Reserve(1000 tones)**	**% B_2O_3**
Turkey	803.000	63
USA	209.000	16.4
USSR	136.000	10.7
Chile	41.000	3.2
China	36.000	2.8
Peru	22.000	1.7
Bolivia	19.000	1.5
Argentina	9.000	0.7
Total	**1.323.000**	**100**

The mineralogical properties of boron minerals present in Turkey are given in Table 1.4 [12].

Boron always maintain its valance state of 3+, therefore tetrahedral bonding has a negative charge and seeks attachment to a cation which helps to make its structure more stable.

The world's largest reserves of borates occur in a 300 km east-west, 150 km north-south, L- shaped area in western Turkey as shown in Figure 1.3. It is south of the Marmara Sea in western Anatolia and 70-100 km east of the Aegean Sea. There are four main borate districts in Turkey, each having different mineralization, but of a similar age, with sediments deposited from inland lakes during active volcanic period.

Table 1.4 The Mineralogical Properties of Important Boron Minerals Present in Turkey[12]

Mineral Name	Color	Density(gr/cm^3)	Hardness
Colemanite **($2CaO.3B_2O_3.5H_2O$)**	White	2.42	4.0
Pandermite **($5CaO.6B_2O_3.9H_2O$)**	White	2.40	3.5
Borax **($Na_2O.2B_2O_3.10H_2O$)**	White	1.70	2.0-2.5
Ulexite **($Na_2O.\ 2CaO\ .5B_2O_3.16H_2O$)**	White	1.65	1.0
Boracite **($6MgO.8B_2O_3.MgCl_2$)**	White	2.90	7.0
Meyerhofferite **($2CaO.3B_2O_3.7H_2O$)**	White	2.12	2.0

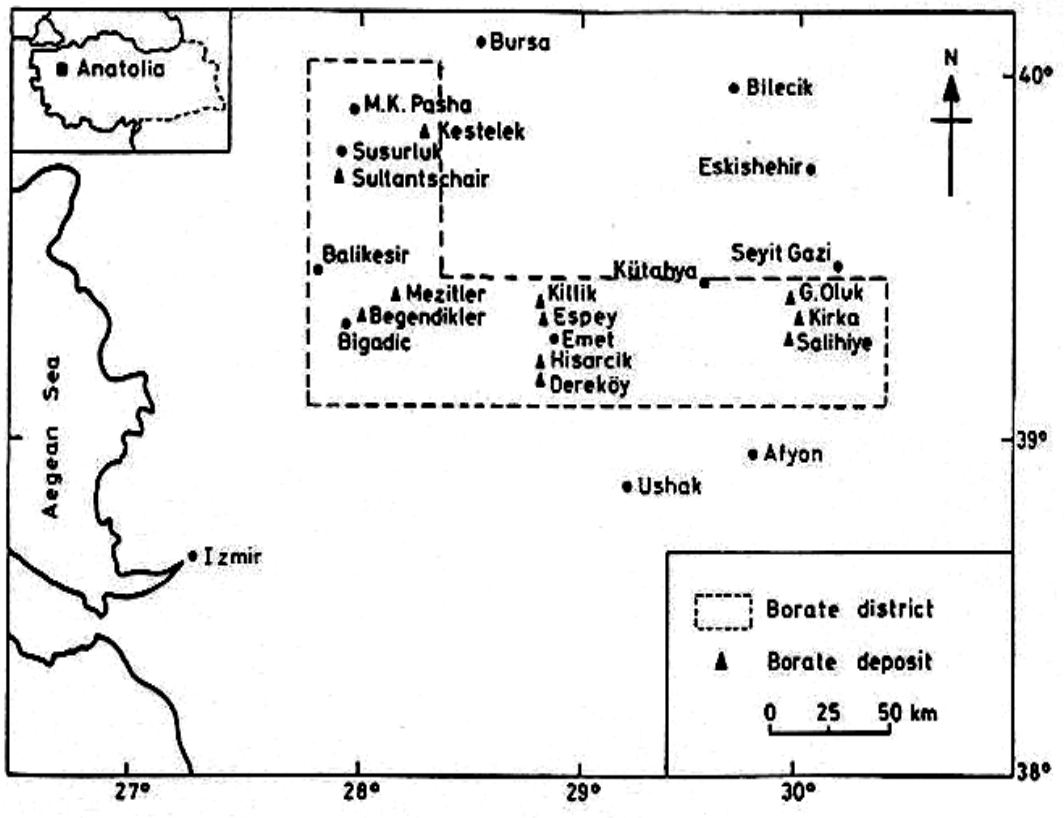

Figure 1.3 Location of the Major Borate Deposits in Turkey[13]

In northwestern corner of this borate district (Bursa), the Sultançayırı deposit contained predominantly gypsium-clay matrix, while nearby, Kestelek has colemanite. Bigadiç, (Balıkesir), in the southwestern corner of the district, has both colemanite and ulexite, while Emet, in Kütahya province, in the south-central district, is similar to Kestelek. Finally, Kırka (Eskişehir) in the southeastern corner contains primarily borax [13]. Kırka, the world's largest borax deposit, is located in western Anatolia 240 km west of Ankara, and in the southeastern corner of the borate district. Colemanite deposits were first discovered at Kırka in 1960. Yet, when the area was more fully drilled, it was found to contain primarily borax, with only secondary colemanite and ulexite. It has around 500.10^6 metric tons of 25% B_2O_3 [14].

1.3. Uses of Boron and Boron-Oxygen Compounds

Boron and its compounds have an unusually large applications from abrasives to wood preservatives, from glass to fuels, from alloys to refractories,etc. [15].

In general, boron reduces the thermal expansion of glass considerably, provides good resistance to vibration, high temperatures and thermal shocks, and improves its toughness, strength, chemical resistance and durability. Boron is the most abundant element after SiO_2 in glasses [16].

There are a large number of commercial applications of borate-containing glasses. For instance, the borosilicate glass used for reaction columns, industrial piping is designed to withstand thermal shock and retain its dimensional stability to 400 ^oC [17]. The mild alkalinity of borax allows it to emulsify oil and greases, and to reduce the surface tension of water, which aids in loosening dirt particles[18]. Moreover, boric acid, borax and pentahydrate have been used to produce inexpensive cellulose insulation material since borates promote the formation of water, which absorbs heat and lowers the temperature during heating. Later it forms a glassy substrate that inhibits burning [19]. Besides these, composites of boron or boride fibers in a matrix of plastics, ceramics or metals have great strength and a high modulus of elasticity [20].

The boride and boron nitride compounds are very hard and are used as abrasives and refractories. Among these, the most important ones for industry are BN (boron nitride), and B_4C (boron carbide).

Another important function of boron is in cell growth and structure. A deficency changes the cell walls, making most of them thinner. Boron is not known to have an essential biochemical function in humans or animals, although one of its functions may be a role in the body's ability to use calcium [20]. Boric acid and sodium borate are mild antiseptics which inhibit gram-negative bacteria, and boric acid has long been used as an eye wash. Some heterocyclic boron compounds inhibit tumor growth, while borax and some of its ores are highly effective in killing parasites [21]. Moreover, in other medical applications, some boron compounds reduce serum cholesterol and other harmful proteins.

Boron and its hydrides have the highest heat of combustion per unit weight of all the elements, 58.4 compared with 43 j/g for aviation gasoline, causing it to be considered as a fuel for aircraft or space [15].

The addition of 0.001% to 0.003% (by weight) boron to steel reduces the amount of nickel, chromium, or molybdenum required [22]. Being small, boron tends to locate in the interstitial space between the metal atoms of the alloy, causing it to be harder and stronger than the parental metal.

In nuclear reactors the fission of radioactive material produces heat and a variety of alpha and beta particles, gamma rays and neutrons. The most effective materials for shielding the neutrons are boron (especially ^{11}B), hydrogen, lithium, polyethylene and water. Most of the shielding materials produce secondary gamma rays, which then require heat removal and further shielding. Boron is unique in its ability to absorb thermal neutrons and produce only a soft gamma ray and an easily absorbed alpha particle. Borates (such as colemanite) can also be added to concrete or structural ceramics to increase their ability to absorb neutrons [23].

1.4. Phosphate Chemistry

Nearly all natural occurring phosphorus compounds are orthophosphate salts. These may contain several different cations as well as other anions and a considerable variety of phosphate minerals have now been characterized. Most of these are comparatively rare, however, the only abundant sources of phosphorus are apatites, $Ca_{10}(PO_4)_6X_2$ (where X is usually OH or F) [24].

The phosphate ion, PO_4^{3-}, is often compared with the silicate, SiO_4^{4-}, sulphate, SO_4^{2-}, and perchlorate, ClO_4^{4-}, ions which have similar tetrahedral configurations. On the basis of classical valency formulations, these XO_4^{4-} ions form a series with an increasing amount of covalent character on going from X=Si to X=Cl [25].

Many compounds in which one or several oxygen atoms of the basic PO_4 building unit are substituted by other atoms as, H, F, or S, must also be considered as phosphates [26].

1.4.1. Classification of Phosphates

Like in all classes of compounds in which the anionic part can condense, the classification of phosphates must be supported by the knowledge of the various geometries of the anions.

The apellation of monophosphates is given to compounds whose anionic entity, $[PO_4]^{3-}$, is composed by an almost regular tetrahedral arrangement of four oxygen atoms centered by a phosphorous atom. The corresponding salts are known as orthophosphates. They are called today as monophosphates.

Among the various categories of phosphates, monophosphates are the most numerous, not only because they were the first to be investigated, but also because they are the most stable and therefore, the only phosphates to be found in nature.

The term condensed phosphates is applied to salts containing condensed phosphoric anions as shown in Figure 1.4.

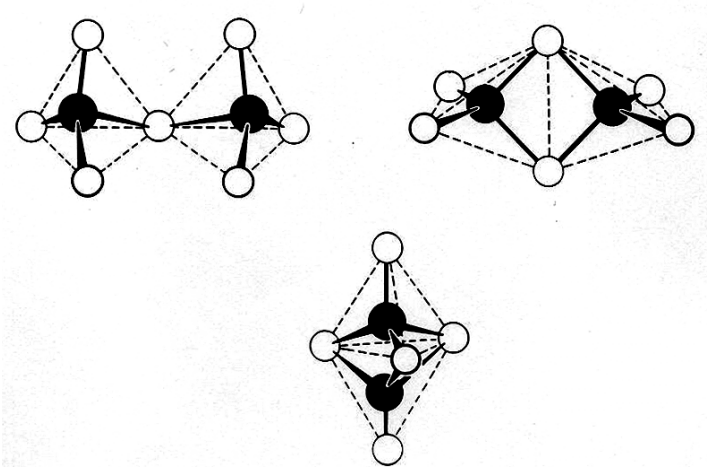

Figure 1.4 Condensed PO_4 Tetrahedra. **a)** Corner Sharing, **b)** Edge Sharing, **c)** Face Sharing [24]

A strict definition of this type of anion can be given by saying that any phosphate anion including one or several P-O-P bonds is a condensed phosphate anion. The formation of these bonds can be performed by many different processes. The simpliest of these processes, commonly used to produce the P_2O_7 diphosphate anion, built by two corner-sharing PO_4 tetrahedra:

$$2Na_2HPO_4 \rightarrow Na_4P_2O_7 + H_2O \text{ (at 700-900 K)}$$

The first type of condensation corresponds to a progressive linear linkage, by corner sharing, of PO_4 tetrahedra, this association leading to the formation of finite or infinite chains. The corresponding phosphates are generally known as *polyphosphates*. The general formula for such anions can be given as $[P_nO3_{n+1}]^{(n+2)-}$ where n is the number of phosphorous atoms in the anionic entity. The first terms of this condensation, corresponding to small values of n, are commonly named *oligophosphates* and are today well characterized up to n=5.

The terminology used for oligophosphates is now well established:

a) For n=2, the anion is $[P_2O_7]^{4-}$ and the corresponding phosphates for a long time called *pyrophosphates* are now designed by the apellation of *diphosphates* [27-36].
b) For n=3, the formula of the anions becomes $[P_3O_{10}]^{5-}$. The former apellation of *tripolyphophates* for the corresponding salts is now replaced by *triphosphates* [37].
c) For n=4, the anion is $[P_4O_{13}]^{6-}$ and the term *tetraphosphate* is now referred to the former *tetrapolyphosphates* [38].

When n becomes very large, the P/O ratio → 1/3 and the anion can be described as an infinite $(PO_3)_n$ chain. The corresponding phosphates are commonly called *long-chain polyphosphates* or more simply *polyphosphates* [26].

The second type of condensation corresponds to the formation of cyclic structure still built by a set of corner-sharing PO_4 tetrahedra leading to the following anionic formula $[P_nO_{3n}]^{n-}$. These rings are now well characterized for n=3, 4, 5, 6, 8, 9, 10 and 12.

In the first two types of condensation, each PO_4 tetrahedron shares no more than two of its corners with the adjacent ones, whereas in this third type some PO_4 groups of the anionic entity share three of their corners with the adjacent ones. This type of condensation occurs in all condensed phosphates whose anionic entities are richer in P_2O_5 than the richest members of the two classes of condensed anions, long-chain anions and ring anions. From this definition, the formulation of the anion is given by:

$$n[PO_3]^- + mP_2O_5 \text{ or } [P_{(2m+n)}O_{(5m+3n)}]^{n-}$$

The corresponding salts are generally called *ultraphosphates*.

The proper definition of an adduct, in the domain of phosphate chemistry, can be formulated as follows. An adduct is a compound including in its atomic arrangement a phosphate anion and in addition another anion or group of anions, phosphoric or not, coexisting as independent units. Independent units mean that, in these salts, the two anionic entities do not share any atom. These additional anions

are various, O^{2-}, OH^{-}, F^{-} (as in Mg_2FPO_4 or $Mg_3(PO_4)_2.MgF_2$), Cl^{-}, Br^{-}, I^{-}, $[NO_3]^{-}$ (as in $Hg_4(NO_3)(PO_4).H_2O$ or $Hg_3PO_4.HgNO_3.H_2O$), $[BO_3]^{3-}$ (as in $Ln_7O_6(BO_3)(PO_4)$ with Ln:La → Dy), $[CO_3]^{2-}$ ($MnNa_3(PO_4)(CO_3)$, $[SO_4]^{2-}$, $[CrO_4]^{2-}$, $[C_2O_4]^{2-}$, or any kind of phosphate or silicate anions [26]. Heterepolyphosphates can be defined by the term heteropolyanion.

1.4.2. Phosphate Deposits in Turkey

Phosphate rock is widely distributed in the former CENTO region (Iran, Pakistan and Turkey) occurring chiefly in rocks.

Phosphate rock is of widespread occurrence in Turkey but only deposits in southeastern Turkey, in the Derik-Mazıdağı region of Mardin Province, are of potential economic importance as a source of phosphate for fertilizer manufacture [39].

1.4.3. Uses of Phosphates

Phosphate compounds are used for domestic purposes. For example, they are very important in fertilizer industry. The most widely used phosphates for cleaners, detergents, dispersants are sodium phosphates.

Different types of phosphate compounds are used in carbonated beverages (phosphoric acid), nutrient supplements (calcium phosphate) , as breaking acids (monocalcium phosphate monohydrate, $Ca(H_2PO_4).H_2O$), cheese emulsifer (disodium phosphate dihydrate, $Na_2HPO_4.2H_2O$) [40].

The anticorrosive properties of phosphate pigments are ascribed to their strong complexing behavior. Complex forming ability increases with increasing phosphate ring size [41].

In addition, phosphate compounds are used for laser materials [40] and for molecular sieve applications.

1.5. Borophosphates

1.5.1. Borophosphate Compounds

Borophosphates, which contain complex anionic structures built of BO_4, BO_3 and PO_4 groups and their partially protonated species, respectively, are the intermediate compounds of the systems M_xO_y-B_2O_3-P_2O_5-(H_2O).

Boron phosphate is a four connective crystalline polymer whose polymorphous structures have been shown by X-ray diffraction to be similar to that of silica as shown in Figure 1.5. The phosphorous-oxygen and boron-oxygen bond lengths are not equal, being 0.155 and 0.144 nm, respectively, and both the boron and the phosphorous atoms are in a tetrahedral coordination [42].

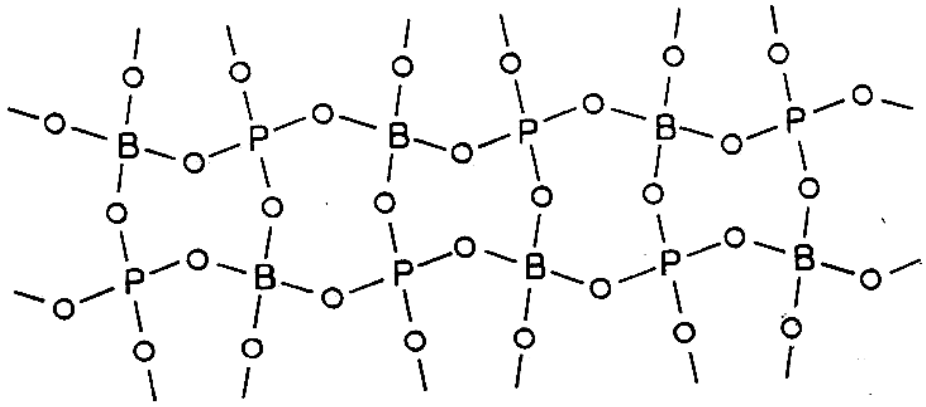

Figure 1.5 Boron Phosphate, Projected on to a Plane [42]

The crystal structures of borophosphates are first divided into anhydrous and hydrated phases [43]. Further gradings are based on the (molar) B:P ratios. Today, the structural chemistry of borophosphate anions already extends from isolated species, oligomers, rings, and chains to layers and frameworks. On the basis of structural classification mentioned above, the following suplementary principles should be pointed out:

1) Compounds with molar ratio B:P>1 contain boron in 3-fold and tetrahedral coordination.
2) Nonbridging corners of borate species in hydrated phases correspond to OH groups.
3) Analogies to the structural chemistry of borates are also given by the frequent formation of 3-membered rings.
4) P-O-P linking is not observed [43].

In recent years, new borophosphates have been widely investigated due to their magnetic, optical and electrooptical applications caused by the primary building units of BO_3, BO_4, and PO_4. $CaBPO_5$ was first prepared by Ramomoorthy and Rockett [44] when investigating 11 binary compounds.

$2MO.B_2O_3.P_2O_5$ (M=Ca, Sr, and Ba) have been first prepared by Bauer [45,46] with thermal methods using the following reactions:

$$CaHPO_4.2H_2O + H_3BO_3 \rightarrow CaBPO_5 + 4\ H_20$$
$$SrCO_3 + H_3BO_3 + (NH_4)_2HPO_4 \rightarrow SrBPO_5 + 3H_2O + CO_2 + 2NH_3$$
$$BaCO_3 + H_3BO_3 + (NH_4)_2HPO_4 \rightarrow BaBPO_5 + 3H_2O + CO_2 + 2NH_3$$

They are found to be isostructural. The cell parameters calculated by Bauer are given in Table 1.5.

Table 1.5 Hexagonal Unit Cell Parameters of $M^{II}BPO_5$ (M^{II}=Ca, Sr, Ba) by Bauer [45,46]

Compound	**a(Å)**	**c(Å)**
$CaBPO_5$	6.688	13.234
$SrBPO_5$	6.857	13.657
$BaBPO_5$	7.111	13.977

Kniep et al. [47] and Gözel [48] synthesized $M[BPO_5]$ and calculated the unit cell dimensions by Rietveld method given in Table 1.6. It was observed that the '**c**' parameter is about the half of the '**c**' given by Bauer.

Table 1.6 Hexagonal Unit Cell Parameters of $M^{II}BPO_5$ (M^{II}=Ca, Sr, Ba) [47,48]

Compound	a(Å)	c(Å)
$CaBPO_5$	6.6799	6.6121
$SrBPO_5$	6.8488	6.8159
$BaBPO_5$	7.1026	6.9821

Synthesis of $SrBPO_5$ [49] and $CaBPO_5$[50] were also reported by Baykal et al. In recent years, $BaBPO_5$ was prepared by using three different methods [51-53].

Liebertz and Stähr [54] in 1982 reported the compound $Mg_3[BPO_7]$ and $Zn_3[BPO_7]$ with α and β structure. The method of synthesis was not given. They indexed both compounds in orthorhombic crystal system. In 1997, Bluhm and Park [55] were able to synthesize single crystals of α-$Zn_3(BO_3)(PO_4)$ at 1050 ^oC by using B_2O_3, P_2O_5 and $ZnCO_3$. They indexed it in monoclinic system. In 2002, Wang and coworkers [56] , growth the single crystal of this compound from melt in hexagonal system. In recent years, Yılmaz et al were able to prepare Co_3BPO_7 by the boron flux method [57].

Gözel [48] also synthesized $M_3[BPO_7]$ (M=Mg, Ba, and Sr) by the solid state reactions given below in the temperature range 700-1500 ^oC and indexed them in the orthorhombic crystal system. The cell parameters and the space groups are given in Table 1.7.

The following solid state reactions were used in the synthesis of M_3BPO_7 (M= Ca, Sr, Ba):

$$MgHPO_4.3H_2O + 2MgCO_3 + H_3BO_3 \rightarrow Mg_3[BPO_7] + 2CO_2 + 5H_2O$$

$$CaBPO_5 + 2CaCO_3 \rightarrow Ca_3[BPO_7] + 2CO_2$$

$$3SrCO_3 + H_3BO_3 + (NH_4)_2HPO_4 \rightarrow Sr_3[BPO_7] + 2NH_3 + 3H_2O + 3CO_2$$

$$3BaCO_3 + H_3BO_3 + (NH_4)_2HPO_4 \rightarrow Ba_3[BPO_7] + 2NH_3 + 3H_2O + 3CO_2$$

Table 1.7 Cell Parameters and the Space Groups of $M_3[BPO_7]$ (M=Mg, Ba, and Sr) Reported By Gözel [48]

Compound	a(Å)	b(Å)	c(Å)	Space Group
α-$Mg_3[BPO_7]$	8.49	4.88	12.55	Pmmm
α- $Sr_3[BPO_7]$	9.0561	9.7984	13.9531	P2/m
α- $Ba_3[BPO_7]$	11.7947	9.6135	12.9548	P2/m

$Na_5[B_2P_3O_{13}]$ was first prepared by high temperature synthesis method and characterized by X-ray single crystal investigations recently by Hauf and coworkers [58]. This compound was also synthesized by using Czochralski method (crystal growth by continious turning and cooling) by Li et al [59]. Besides these, many other borophosphate compounds with the anion groups $[BP_3O_{14}]^{10-}$ [60], $[O_6(BO_3)(PO_4)_2]^{21-}$ [61], $[BP_3O_{12}]^{6-}$ [47, 62], and $[BP_2O_8]^{3-}$ [63] were synthesized by many research groups.

Other than the above borophosphate compounds, there are few hydrated borophosphate compounds; such as $M^IM^{II}(H_2O)_2[BP_2O_8].H_2O$ (M^I=Na, K; M^{II}= Mg, Mn, Fe, Co, Ni, Zn) [64], and $NH_4Mg(H_2O)_2[BP_2O_8].H_2O$ [65], $Fe(H_2O)_2BP_2O_8.H_2O$ [66], $NH_4[(Zn_{1-}xCo_x)BP_2O_8]$ ($0<x<0.14$) [67], $NaZn(H_2O)_2[BP_2O_8].H_2O$ [68], $NH_4M^{III}[BP_2O_8(OH)]$ (M= V or Fe) [69], $(NH_4)_{0.4}Fe^{II}_{0.55}Fe^{III}_{0.5}(H_2O)_2[BP_2O_8].0.6H_2O$ and $NH_4Fe^{III}[BP_2O_8(OH)]$ [70], $(NH_4)_x(H_2O)_2(Co_{((3x-2)/2)}[BP_2O_8].(1-x)H_2O$ (x~0.5) [71], $[(VO)_{12}(O_3POB(O)_2OPO_3)_6]^{18-}$ [72], $(NH_4)_5[V_3BP_3O_{19}].H_2O$ [73], $(Ni_{3-x}Mg_x)[B_3P_3O_{12}(OH)_6].6H_2O$ (x=1.5) [74], $Fe(B_2P_2O_7(OH)_5)$ [75], $(NH_4)_2(C_2H_{10}N_2)_6[Sr(H_2O)_5]_2[V_2P_2BO_{12}]_6.10H_2O$ [76], $(C_4N_2H_{12})Co[B_2P_3O_{12}(OH)]$ [77], $[Co(en)_3][enH_2](V_3BP_3O_{19}).4.5H_2O$ [78], $[Co(en)_3][B_2P_3O_{11}(OH)_2]$ [79], and $(C_3N_2H_5)_8$ $[Mo^V_5Mo^{VI}_7O_{22}(BO_4)_2(PO_4)_5(HPO_4)_3]$ $.nH_2O(n=4)$ [80].

1.5.2. Borophosphate Minerals

The borates are among the most interesting of the world's industrial minerals, which have been known and used since the earliest recorded history, first for

precious metal working and later in ceramics. They are unusually large group of minerals, but the number of commercially important borates is limited, and their chemistry and crystal structure are both unusual and complex.

Although boron is 27th element in abundance, about 230 naturally occurring borate minerals were identified as of 1996 and the increasing sophisticated analytical instruments, computer assistance, and crystallographic identification ensures that many new ones will be found in the future [15].

Among the 230 borate minerals, two minerals contain phosphate groups. These are luneburgite and seamanite which are found in the form of $Mg_3(PO_4)_2[B_2O(OH)_4].6H_2O$, $3MgO.P_2O_5.B_2O_3.8H_2O$, $Mg_3(PO_4)_2B_2O_3.8H_2O$ and $Mn_3^{2+}(OH)_2[B(OH)_4]PO_4$, $6MnO.P_2O_5.B_2O_3.6H_2O$, $Mn_3PO_4BO_3.3H_2O$, respectively. The luneburgite contains dimeric tetrahedra units $[BPO_7]^{6-}$ [81], while the crystal structure of seamanite contains isolated BO_4 and PO_4 tetrahedra [82].

1.3.3. Uses of Borophosphates

Borophosphate glasses have been developed recently for their fast ion conducting and having low melting glass solders capability [83]. Koudelka and co-workers studied the effect of B_2O_3 addition to ZnO-B_2O_3-P_2O_5 on the glass transition temperature and thermal expansion coefficient of borate phosphates [84].

BPO_4 itself is a catalyst used industrially for many reactions including hydration, dehydration, and oligomerization [85].

$MBPO_5$ powders (less than 10 μ diameter, especially $CaBPO_5$), which are uniformly distributed in a polymer binder (e.g.alkydresin acrylate), are used for corrosion protection of metal surfaces [41,86]. Optionally, the protection mixture also contains other binders (e.g. lacquers) and pigments. Different types of metal borophosphate are being used as antioxidants, fire proofing agents (Na, K borophosphate), or binders [87].

Moreover the unusual structural configuration of alkaline earth borophosphates lead to zeolite-like properties, with potential applications as bioceramics for molecular sieves [88]. The most notable trend in the field of molecular sieve synthesis in the past few years in the profound expansions of the variety of studied systems and the rapidly growing number of acronyms associated with them. It is likely that the organic template can be removed from similar compounds and that the channels can then be used for appropriate catalytic reactions. The presence of boron at relatively high concentrations should improve the catalytic properties of such catalysts [85].

Recently, optical [89-93], second harmonic generation [94], and, luminescence [95-99] behaviour of several borophosphate and rare-earth doped borophosphate compounds were studied by several researchers.

Lithium borophosphate, Li-doped BPO_4 is used in the solid state rechargeable lithium ion battery. For this reason, many researchers studied this subject [100-102].

Laser action of Nd and Pr doped zinc chloride borophosphate glass were investigated by Surana [103] and Sharma [104].

BPSG (borophosphosilicate glass) thin films [105-108] are utilized in semiconductor technology as premetal dielectric for insulation.

1.4. Purpose of the Work

Investigation of borophosphates have been carried out in our laboratory for several years by Kızılyallı and coworkers. Recently the results of a research of borophosphosphates of Na, Ca, NH_4, Fe, Sr, Mg and Co compounds were reported [47, 48, 49, 50, 57, 58, 65, 66, 109]. The formation of possible solid solutions with alkaline earth and transition metal borophosphates would be interesting since both borates and phosphates have several uses in technological materials.

The boron and phosphate combination seems to be suitable for the formation of B-O and P-O bonds in either trigonal planar or tetrahedral coordination. In this combination, M:B:P (M=alkaline, alkaline earth or rare earth metals) is important. For some compositions they form a structure which is chemically and thermally stable. On the other hand some borophosphate compounds have an open three dimensional structure framework of corner shared BO_4 and PO_4 tetrahedra.

In this thesis our aim was to investigate the solid-state reactions of alkaline earth carbonates, transition metal oxide (ZrO_2) with B_2O_3(or H_3BO_3) and ammonium phosphates ($(NH_4)_2HPO_4$ or $NH_4H_2PO_4$) at high temperatures in the range 400-1200 ^oC. We are also interested in the behaviour of SiO_2 as p-group oxide in these type of high temperature reactions since no research in this field was reported before. The formulas are given as $M^{IV}O_2.M^{II}O.B_2O_3.P_2O_5$ depending on IUPAC notation for the new compounds with oxide ingredients. The phases were characterized by XRD and IR methods firstly, at the end of each heat treatment samples were examined with XRD and IR analyses. The DTA and EDX analyses were performed in case of borophosphate formation.

CHAPTER II

EXPERIMENTAL TECHNIQUES

2.1. Chemical Substances

The following solid powders were used in the solid state reactions of various metal oxides:

Al_2O_3, B_2O_3, $CaCO_3$, H_3BO_3, Na_2CO_3, $NH_4H_2PO_4$, $(NH_4)_2HPO_4$, SiO_2, $SrCO_3$, ZrO_2 (From Merck, Aldrich, Sigma and Riedel).

2.2. Instrumentation

a) X-Ray Diffractometer

X-ray powder diffraction patterns (XRD) were taken by using Philips diffractometer with PW 1050/25 goniometer and Co (Kα 30-40 kV, 10-20 mA, λ=1.79021Å) radiation and Huber Diffractometer with Cu ($K\alpha_1$ 30-40 kV, 10-20 mA, λ=1.54056Å). Scanning was generally done between 6-70 degree 2 Theta.

b) Infrared Spectrophotometer

Nicolet 510 FTIR Infrared Spectrometer was used in the region 400-4000 cm^{-1}. Spectroscopic grade KBr was used for making IR pellets. It was dried at 180 ^oC for about 2 hours before using. Spectra of solids were obtained from KBr pellets using KBr:Sample ratio=100mg:3mg.

c) Energy Dispersive X-ray Analyzer (EDX)

The quantitative analysis of Sr, Zr, P have been done with Energy Dispersive X-ray Analyzer (EDX) (20kV) which is attached to a Scanning Electron Microscope.

d) Differential Thermal Analyzer (DTA)

Thermal behaviour of specimens was examined by Dupont thermal analyst 2000 DSC 910S model differential scanning calorimeter. About 5 mg of the specimens was inserted to the instrument and heated by 10 ^{o}C/min.

e) Furnaces

The solid state reactions have been carried out in air with the aid of Heraous (KR-170), SFL West-6100 and Neyo 2-525 (computer controlled) furnaces. Heating ranges were 550-1200 ^{o}C, 300-1200 ^{o}C and 300-900 ^{o}C respectively using Cr-Ni-Cr and Rh-Pt-Rh thermocouples.

2.3. Experimental Procedure

In this study, solid powder samples of about 2.5-5 grams are weighted and blended thoroughly in an agate mortar and placed in convenient porcelain crucible or boat. This mixture then heated in one of the furnaces mentioned above at desired temperatures and time intervals. To avoid melting, reactions started at room temperature and temperature was increased to 400 ^{o}C gradually. At each step, samples are taken out of the furnace and cooled. After cooling they were blended again to homogenize the mixture. Heating process was repeated to complete the reaction. At the end, the reaction products were examined using various analytical techniques.

The types of reactions, solid state, flux, hydrothermal are given below.

2.3.1. Solid State Reactions

Reactions of various metal oxides were first performed by solid state techniques. Each reaction is characterized by an experiment number which is given in the text as **Exp.No.** and comma used for successive heat treatments at different temperatures and time intervals.

The reactants were dried in an oven at 50 ^{o}C then were mixed in the required proportions in an agate mortar and the mixtures were heated (in some cases with 2K/min heating rate) at different temperatures in the range 400-1200 ^{o}C in porcelain crucibles.

2.3.1.1. Solid State Reactions of $2ZrO_2 + 2SrCO_3 + B_2O_3$ with $2(NH_4)_2HPO_4$

Two different methods were used for the solid state reactions. In each case at least one of the reactants was different.

In the solid state reactions, reactants were used in the ratio of $2ZrO_2$:$2SrCO_3$: B_2O_3:P_2O_5(as $2(NH_4)_2HPO_4$). In these reactions NH_3(g), H_2O(g), and CO_2(g) are evolved at high temperatures.

$2ZrO_2(s) + 2SrCO_3(s) + B_2O_3(s) + 2(NH_4)_2HPO_4(s)$ **(Exp.No:D5)**

The experimental conditions are given in Table 2.1.

Table 2.1 The Experimental Conditions for the Solid State Reactions of $2ZrO_2 + 2SrCO_3 + B_2O_3 + 2(NH_4)_2HPO_4$

Exp.No	Temp. (^{o}C)	Duration (h)
D5.1	900	14.5
D5.2	950	36.5
D5.3	1100	5
D5.4	1200	5

In the second method, boron flux technique was employed using different phosphating agents [$(NH_4)_2HPO_4$ or $NH_4H_2PO_4$] and excess B_2O_3 or H_3BO_3. In flux reactions, one or more reactants are used as an excess. Then this mixture is heated directly to higher temperatures (>1000 ^oC) to melt the mixture. Then, the products are cooled slowly to obtain single crystals.

The compositions were as follows:

$2ZrO_2(s) + 2SrCO_3(s) + 12B_2O_3(s) + 2(NH_4)_2HPO_4(s)$ **(Exp.No:D45)**

$2ZrO_2(s) + 2SrCO_3(s) + 12B_2O_3(s) + 2NH_4H_2PO_4(s)$ **(Exp.No:D46)**

$2ZrO_2(s) + 2SrCO_3(s) + 12H_3BO_3(s) + 2(NH_4)_2HPO_4(s)$ **(Exp.No:D47)**

$2ZrO_2(s) + 2SrCO_3(s) + 12H_3BO_3(s) + 2NH_4H_2PO_4(s)$ **(Exp.No:D48)**

The conditions given in Table 2.2 were used for these reactions.

Table 2.2 The Experimental Conditions for Boron Flux Reactions (The Temperatures and Heating Times Were Given In Order)

Exp.No	Temp. (^oC)	Duration (h)
D45	400/700/850/910/950/1000/1040/1200	3.5/16/5/5.5/5/4/5/5
D46	400/700/850/910/950/1000/1040/1200	3.5/16/5/5.5/5/4/5/5
D47	400/700/850/910/950/1000/1040/1200	3.5/16/5/5.5/5/4/5/5
D48	400/700/850/910/950/1000/1040/1200	3.5/16/5/5.5/5/4/5/5

2.3.1.2. Solid State Reactions of $2SiO_2 + 2SrCO_3 + B_2O_3$ with $2(NH_4)_2HPO_4$

The reactants $2SiO_2$, $2SrCO_3$, B_2O_3, and $2(NH_4)_2HPO_4$ were heated to temperatures given in Table 2.3 and kept at that temperature for the given durations.

Table 2.3 The Experimental Conditions for the Solid State Reactions of $2SiO_2$ + $2SrCO_3$ + B_2O_3 + $2(NH_4)_2HPO_4$

Exp.No	Temp. (^oC)	Duration (h)
D9.1	900	14.5
D9.2	950	36.5
D9.3	1100	5

2.3.1.3. Solid State Reactions of $2ZrO_2 + 2CaCO_3 + B_2O_3$ with $2(NH_4)_2HPO_4$

In the case of Ca^{2+}, depending on the inital experiments, two different methods were used:

a) ZrO_2, $CaCO_3$, B_2O_3, and $(NH_4)_2HPO_4$ in the molar ratio 2:2:1:2 was heated in the range 900-1200 ^oC. The conditions are given in Table 2.4 **(Exp.No:D2)**.

b) In the second method, the amount of phosphating agent was increased since it was observed that the amount of it was not enough **(Exp.No:D3)**.

The composition and heating procedure for the reactions are given in Table 2.4.

Table 2.4 The Experimental Conditions for the Solid State Reactions of $2ZrO_2$ + $2CaCO_3$ + B_2O_3 + $2(NH_4)_2HPO_4$

Exp.No	Temp. (^oC)	Duration (h)	Compostion
D2	900	12	2:2:1:2
D2A	950	14	2:2:1:2
D2B	900/950/1100	12/28/6	2:2:1:2
D3	900	12	2:2:1:4
D3A	950	14	2:2:1:4
D3B	900/950/1100	12/28/6	2:2:1:4

2.3.1.4. Solid State Reactions of $2Al_2O_3 + B_2O_3$ with $2(NH_4)_2HPO_4$

In this experiment, the following composition was used:

$2Al_2O_3(s) + B_2O_3(s) + 2(NH_4)_2HPO_4(s)$ **(Exp.No:D1)**

The heating temperatures given in Table 2.5 were used for this experiment.

Table 2.5 The Experimental Conditions for the Solid State Reactions of $2Al_2O_3 + B_2O_3 + 2(NH_4)_2HPO_4$

Exp.No	Temp. (^oC)	Duration (h)
D1.1	900	12
D1.2	950	28
D1.3	1100	7

2.3.1.5. Solid State Reactions of H_3BO_3 and B_2O_3 with $(NH_4)_2HPO_4$

In these reactions, boron oxide and boric acid were treated with $(NH_4)_2HPO_4$. The ratio of B:P was taken as 3:1 to investigate the formation of a possible borophosphates other than BPO_4 where B:P is 1:1.

The heating procedure applied for these reactions is summarized in Table 2.6.

Table 2.6 The Experimental Conditions for the Solid State Reactions of H_3BO_3 and B_2O_3 with $(NH_4)_2HPO_4$

Exp.No	Temp. (^oC)	Duration (h)	Composition
K1	400/500/600/700/800	5/5/5/5/6	$3B_2O_3+2(NH_4)_2HPO_4$
K2	950	9	$3B_2O_3+2(NH_4)_2HPO_4$
B3	500/700/900/950	5/5/10/4	$3H_3BO_3+(NH_4)_2HPO_4$

2.3.1.6. Solid State Reactions of ZrO_2+Na_2CO_3+H_3BO_3 with $NH_4H_2PO_4$

ZrO_2, Na_2CO_3, H_3BO_3, and $NH_4H_2PO_4$ in the molar ratio 1:1:1:1 was heated up to 910 ^oC since it is the optimum temperature for sodium zirconium phosphate formation [110]. The following composition was used:

$ZrO_2(s) + Na_2CO_3(s) + H_3BO_3(s) + NH_4H_2PO_4(s)$ **(Exp.No:D53)**

The heating conditions are given in Table 2.7.

Table 2.7 The Experimental Conditions for the Solid State Reactions of ZrO_2 + Na_2CO_3 + H_3BO_3 + $NH_4H_2PO_4$

Exp.No	Temp. (^oC)	Duration (h)
D53.1	500	5
D53.2	730	5
D53.3	750	5
D53.4	850	5.5
D53.5	880	5
D53.6	910	5.5

2.3.2. Hydrothermal Reactions

Hydrothermal reactions are carried out in the aqueous medium and relatively high pressure conditions. In this case, stoichiometric amount of chemicals were put into a 50 ml beaker, H_3PO_4 water mixture were added dropwise in order to dissolve the solid mixture completely in a minimum amount of solution. After dissolving the solid completely, the volume of solution was adjusted to 15 ml by evaporating. The pH of the final solution was 1.4. The solution was poured into a Teflon autoclave, closed very tightly, and heated at 150 ^oC in an oven and kept at that temperature for 12 days. After the heating process, the autoclave was taken out of the oven and opened. In order to take its solid content, it was filtered (by Whatman 40 filter paper) and washed with distilled water several times. The precipitate was heated in an oven

at 100 ^{o}C for a short time. After this process, XRD pattern and IR spectrum of the sample were recorded.

2.3.2.1. Hydrothermal Reactions of $ZrO_2 + SrCO_3 + H_3BO_3 + (NH_4)_2HPO_4$

In this experiment, ZrO_2 were used as a source of Zr, $SrCO_3$ for Sr, H_3BO_3 for B and $(NH_4)_2HPO_4$ for P and H_3PO_4 was used as an acid. The experimental procedure for the hydrothermal reactions of $ZrO_2 + SrCO_3 + H_3BO_3 + (NH_4)_2HPO_4$ is given in Table 2.8. To see the changes in the XRD patterns, products were heated to 1100 and 1200 ^{o}C according to result of DTA measurements.

Table 2.8 The Experimental Procedure for the Hydrothermal Reactions of $ZrO_2 + SrCO_3 + H_3BO_3 + (NH_4)_2HPO_4$

Exp.No	**Composition Zr:Sr:B:P**	**Duration (Day)**	**Temperature (^{o}C)**
D44	1:1:1:1	12	150

CHAPTER III

RESULTS AND DISCUSSION

3.1. Solid State Reactions

3.1.1. Solid State Reactions of $2ZrO_2 + 2SrCO_3 + B_2O_3$ with $2(NH_4)_2HPO_4$

Reactions with the composition given below were performed at 900, 950, 1100 and 1200 ^oC as given in Table 2.1 (page 23) and XRD patterns were taken.

$2ZrO_2(s) + 2SrCO_3(s) + B_2O_3(s) + 2(NH_4)_2HPO_4(s) \rightarrow 2ZrO_2.2SrO.B_2O_3.P_2O_5(s) + 4NH_3(g) + 3H_2O(g) + 2CO_2(g)$ **(Exp.No:D5)**

In this reaction, which was performed at 950 ^oC (**Exp.No:D5.2**), $SrBPO_5$ (J.C.P.D.S. Card. No:18-1270 in Appendix A) was obtained together with unreacted ZrO_2 (J.C.P.D.S. Card No: 37-1484 in Appendix B) and $Sr_7Zr(PO_4)_6$ (J.C.P.D.S. Card No:34-65 in Appendix C). The X-ray powder diffraction pattern of the products obtained in **Exp.No:D5.2** is given in Figure 3.1. Table 3.2 gives remarks on the X-ray powder diffraction data of the products obtained from the reactions of $2ZrO_2 + 2SrCO_3 + B_2O_3 + 2(NH_4)_2HPO_4$. Although there are d-spacings belonging to $SrBPO_5$, ZrO_2, $Sr_7Zr(PO_4)_6$, there are some other d-spacings which were indexed in orthorhombic system with a=11.85Å, b=12.99 Å, c=17.32 Å.

This indexed pattern of the product is expected to be related with a new phase. The indexed pattern has some common lines with $Sr_7Zr(PO_4)_6$ and ZrO_2. This structural similarity would be proved after obtaining single crystal of $SrZr[BPO_7]$ by using hydrothermal or flux method.

The EDX analysis of the products obtained from the reaction of $2ZrO_2$ + $2SrCO_3$ + B_2O_3 with $2(NH_4)_2HPO_4$ showed the presence of Zr, Sr, and P elements as shown in Figure 3.2.

The IR spectrum, given in Figure 3.3, of the products obtained from **Exp.No:D5.2** showed that the bands matched with the IR spectrum of $SrBPO_5$ [41,86]. Table 3.2 indicates the observed bands with assignments of **Exp.No:D5.2** and **D9.2**. The extra bands (901, 504, 421 cm^{-1}) are due to $Sr_7Zr(PO_4)_6$ and ZrO_2. The same bands were observed for $SrBPO_5$ in the IR spectrum of the product for the experiment done by SiO_2 instead of ZrO_2 (**Exp.No:D9.2**). This was also included in Table 3.1 for the purpose of comparison.

The theoretical and the experimental percent weight losses are in agreement, being 24.02 % and 27.55 %, respectively.

Table 3.1 The IR frequencies of the Products Obtained From the Solid State Reactions of $2ZrO_2$ + $2SrCO_3$ + B_2O_3 with $2(NH_4)_2HPO_4$ and SiO_2 + $SrCO_3$ + B_2O_3 with $(NH_4)_2HPO_4$ at 950 ^oC **Exp.No:D5.2** and **D9.2**, respectively

Assignments	**$SrBPO_5$(cm^{-1})[49]**	**D5.2(with ZrO_2)**	**D9.2(with SiO_2)**
ν (P=O)	1216	1209	1208
ν_3 (BO_4)	1117	1110	1110
ν_3 (PO_4)	1051	1044	1046
ν_1 (PO_4)	972	978	972
ν_{as} (BOP)	850/800	863/810	863/814
ν_s (BOP)	749	754	754
δ (BOP)	655	656	656
δ (OPO)	561	558	560
δ (BO_4)	519/466	524	529
ν_4 (PO_4)	466	469	469

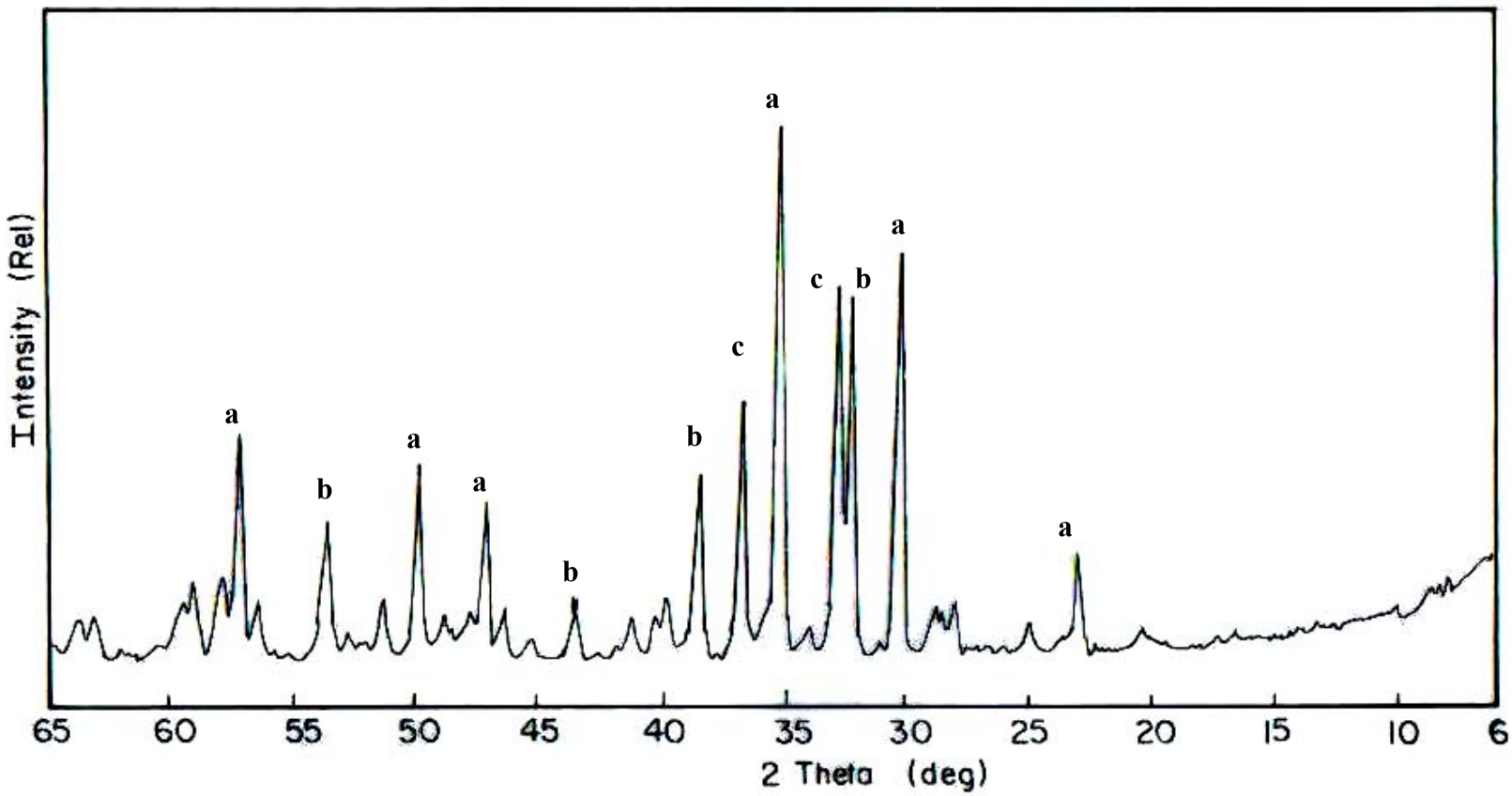

Figure 3.1 The X-ray Powder Diffraction Pattern of the Products Obtained From the Solid State Reactions of $2ZrO_2 + 2SrCO_3 + B_2O_3$ with $2(NH_4)_2HPO_4$ at 950 ^oC (where a= S B c r

Table 3.2 The X-ray Powder Diffraction Data of the Products Obtained From the Solid State Reactions of $2ZrO_2 + 2SrCO_3 + B_2O_3$ with $2(NH_4)_2HPO_4$ at 950 ^oC. The S BP pound was indexed with a=11.85Å, b=12.99 Å, c=17.32 Å in o rh stem

I/I_o	d_{obs}	d_{cal}	$\sin^2\theta_{obs}$	$\sin^2\theta_{cal}$	hkl	Remarks
4	12.9940	12.9900	0.00475	0.00475	010	
2	5.9345	5.9250	0.02275	0.02282	200	
2	5.1042	5.1472	0.03075	0.03024	211	
19	4.4897	4.5765	0.03975	0.03825	212	**$SrBPO_5$**
8	4.1602	4.1350	0.04629	0.04686	203	**$Sr_7Zr(PO_4)_6$**
12	3.7130	3.6923	0.05812	0.05877	311	
4	3.6426	3.6813	0.06038	0.05912	132	
4	3.6054	3.6028	0.06164	0.06173	024	**$Sr_7Zr(PO_4)_6$**
77	3.4300	3.4268	0.06786	0.06823	231	**$SrBPO_5$**
2	3.3495	3.3470	0.07142	0.07152	015	
69	3.2180	3.2210	0.07737	0.07723	115	**$Sr_7Zr(PO_4)_6$**
71	3.1703	3.1620	0.07972	0.07972	313	**ZrO_2**
6	3.0659	3.0618	0.08524	0.08547	034	**$SrBPO_5$**
100	2.9603	2.9596	0.09143	0.09147	125	**$SrBPO_5$**
46	2.8470	2.8472	0.09885	0.09883	314	**ZrO_2**
36	2.7218	2.7200	0.10815	0.10829	234	**$Sr_7Zr(PO_4)_6$**
11	2.6329	2.6358	0.11558	0.11533	403	**ZrO_2**
7	2.6077	2.6044	0.11782	0.11812	305	**ZrO_2**
7	2.5984	2.5980	0.11867	0.11871	050/044	
8	2.5500	2.5448	0.12322	0.12372	216	
12	2.4209	2.4210	0.13671	0.13670	431	
5	2.3366	2.3481	0.14676	0.14531	501	
10	2.2768	2.2859	0.15456	0.15333	502	**$SrBPO_5$**
29	2.2425	2.2514	0.15932	0.15807	512	**$SrBPO_5$**
3	2.2137	2.2184	0.16349	0.16281	415	**ZrO_2**

Table 3.2 Continued

4	2.1668	2.1650	0.17066	0.17094	060	**$Sr_7Zr(PO_4)_6$**
35	2.1300	2.1298	0.17661	0.17664	160	**$SrBPO_5$**
11	2.0754	2.0773	0.18602	0.18567	523	**$Sr_7Zr(PO_4)_6$**
4	2.0238	2.0215	0.19562	0.19606	532	
25	1.9956	1.9975	0.20119	0.20080	435	**$Sr_7Zr(PO_4)_6$**
7	1.8957	1.8985	0.22294	0.22229	360	**$SrBPO_5$**
40	1.8744	1.8741	0.22805	0.22811	534	**$SrBPO_5$**
14	1.8507	1.8503	0.23393	0.23403	453	**$Sr_7Zr(PO_4)_6$**
14	1.8178	1.8171	0.24248	0.24265	543	**ZrO_2**
9	1.7107	1.7134	0.27378	0.27291	462	**$SrBPO_5$**
8	1.6962	1.7010	0.27846	0.27693	615	**ZrO_2**
11	1.6614	1.6624	0.29027	0.28991	266	**$SrBPO_5$**
12	1.6479	1.6563	0.29504	0.29206	642	**$SrBPO_5$**
7	1.6111	1.6173	0.30866	0.30631	616	**ZrO_2**
5	1.5684	1.5658	0.32571	0.32678	651	**$Sr_7Zr(PO_4)_6$**

($SrBPO_5$) (J.C.P.D.S. Card. No:18-1270 in Appendix A)

ZrO_2 (J.C.P.D.S. Card No: 37-1484 in Appendix B)

$Sr_7Zr(PO_4)_6$ (J.C.P.D.S. Card No:34-65 in Appendix C)

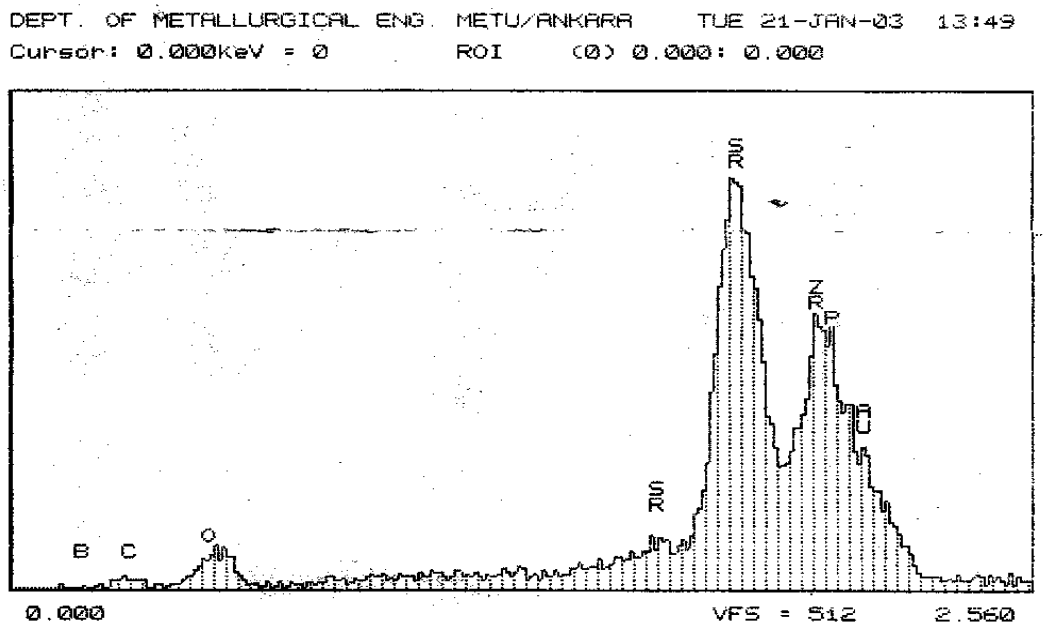

Figure 3.2 EDX Spectrum of the Products Obtained From the Reaction of $2ZrO_2$ + $2SrCO_3$ + B_2O_3 with $2(NH_4)_2HPO_4$ at 950 ^oC

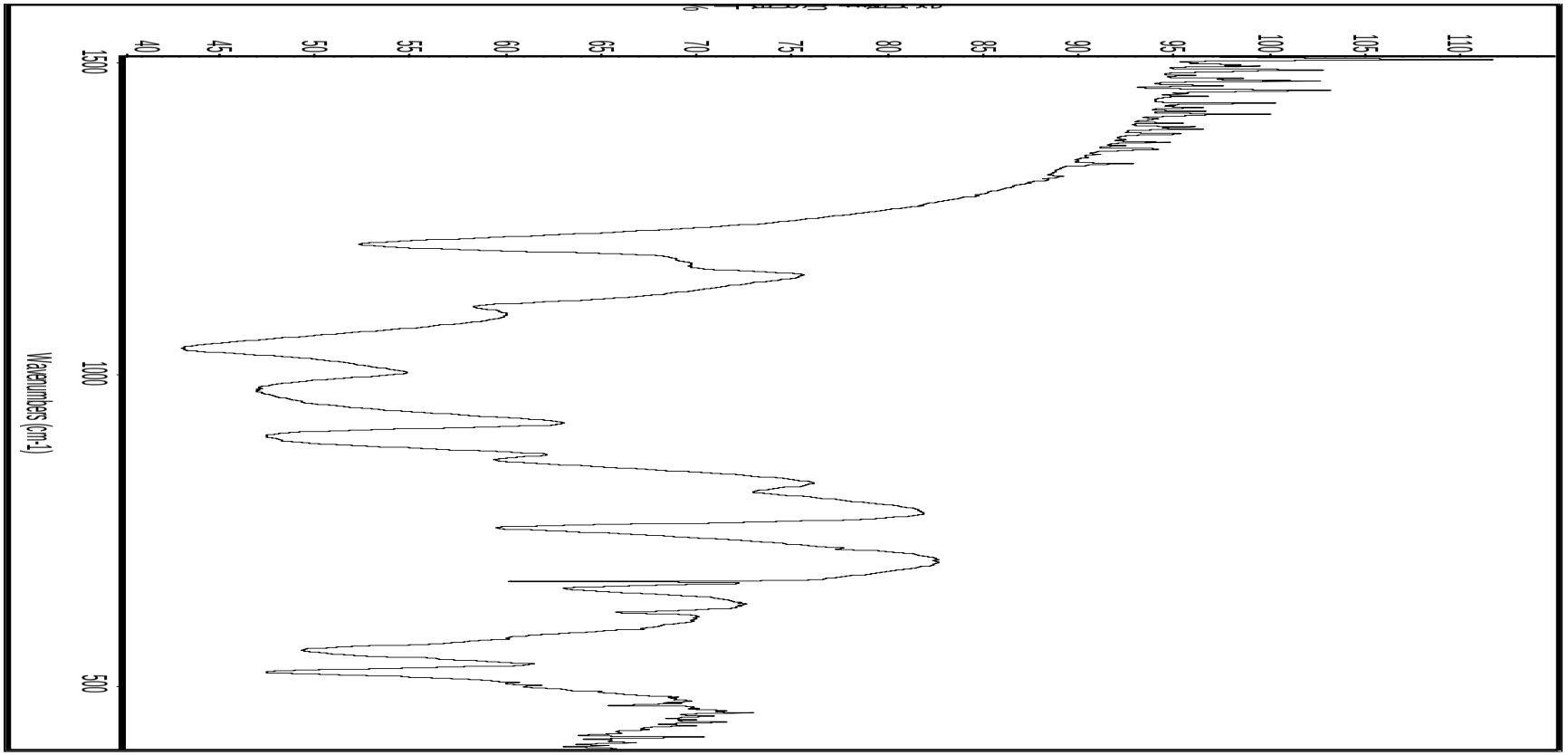

Figure 3.3 The IR Spectra of the Products Obtained From the Solid State Reactions of $2ZrO_2$ + $2SrCO_3 + B_2O_3$ $_4)_2HPO_4$ at 950 ^oC

Since there are many phases in the products of **Exp.No:D5.2**, the sample was heated at 1100 ^{o}C to see the changes in d-spacings. At 1100 ^{o}C, mainly $Sr_7Zr(PO_4)_6$ was observed in the X-ray diffraction pattern of the product (Figure 3.4). Table 3.3. gives X-ray diffraction data of the products obtained at 1100 ^{o}C. The unknown peaks were found to be stronger than the known ones which was reported before in the case of the product obtained at 950 ^{o}C.

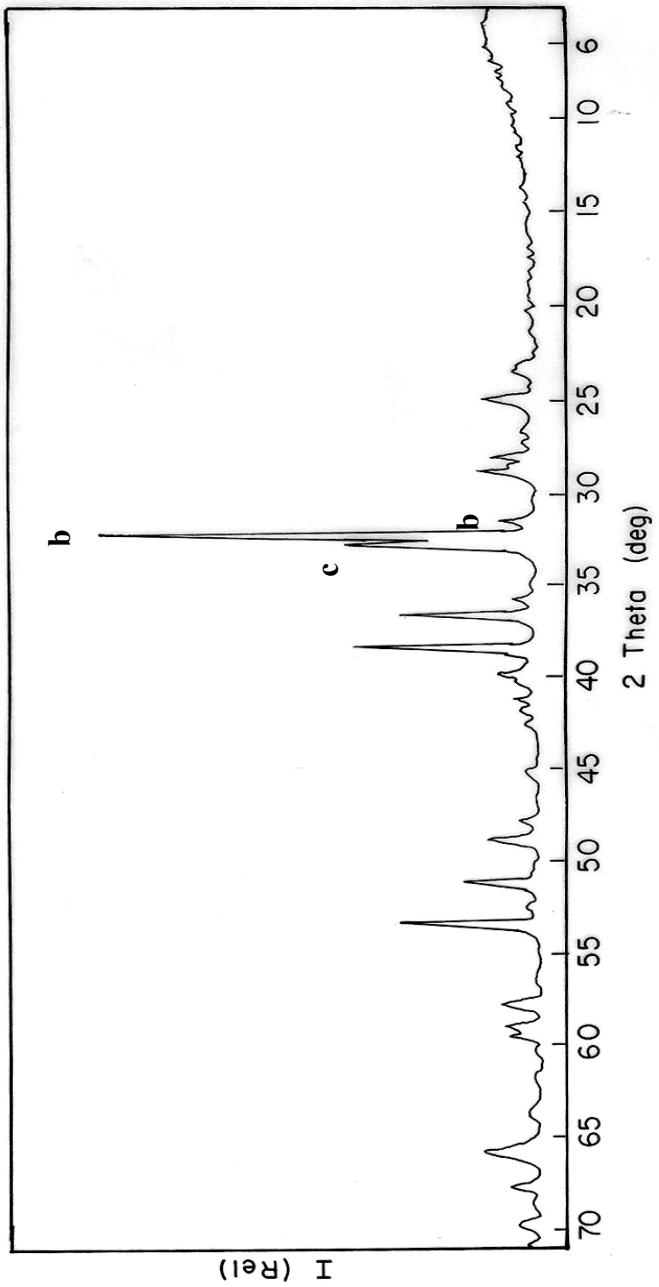

Figure 3.4 The X-ray Powder Diffraction Pattern
Reactions of 2ZrO $_3$ + B_2O_3 with 2(NH)
b=$Sr_7Zr(PO_4$

Table 3.3 The X-ray Powder Diffraction Data of the Products Obtained From the Solid State Reactions of $2ZrO_2 + 2SrCO_3 + B_2O_3$ with $2(NH_4)_2HPO_4$ at 1100 ^oC

I/I_o	d_{obs}	Remarks	I/I_o	d_{obs}	Remarks
6	4.4705	**unknown**	4	2.3341	**ZrO_2**
6	4.4515	**unknown**	5	2.2094	**ZrO_2**
6	4.4140	**unknown**	10	2.1647	**$Sr_7Zr(PO_4)_6$**
12	4.1519	**$Sr_7Zr(PO_4)_6$**	17	2.0716	**$Sr_7Zr(PO_4)_6$**
2	3.8838	**$Sr_7Zr(PO_4)_6$**	2	2.0238	**ZrO_2**
8	3.7000	**$Sr_7Zr(PO_4)_6$**	32	1.9904	**ZrO_2, $Sr_7Zr(PO_4)_6$**
6	3.6364	**ZrO_2**	2	1.8850	**unknown**
14	3.5932	**$Sr_7Zr(PO_4)_6$**	10	1.8492	**ZrO_2**
9	3.3027	**$Sr_7Zr(PO_4)_6$**	8	1.8178	**ZrO_2**
100	3.2180	**$Sr_7Zr(PO_4)_6$**	7	1.8039	**ZrO_2**
43	3.1703	**ZrO_2**	1	1.7507	**unknown**
1	3.0880	**unknown**	2	1.7430	**$Sr_7Zr(PO_4)_6$**
6	2.9123	**unknown**	1	1.7010	**ZrO_2**
32	2.8432	**ZrO_2**	1	1.6939	**ZrO_2**
41	2.7150	**$Sr_7Zr(PO_4)_6$**	14	1.6490	**$Sr_7Zr(PO_4)_6$**
10	2.6234	**ZrO_2**	14	1.6457	**$Sr_7Zr(PO_4)_6$**
3	2.6046	**ZrO_2**	8	1.6059	**$Sr_7Zr(PO_4)_6$**
6	2.5411	**ZrO_2**	2	1.5904	**ZrO_2**
4	2.5063	**ZrO_2**	6	1.5674	**$Sr_7Zr(PO_4)_6$**
3	2.4586	**unknown**	5	1.5433	**ZrO_2**

ZrO_2 (J.C.P.D.S. Card No: 37-1484 in Appendix B)

$Sr_7Zr(PO_4)_6$ (J.C.P.D.S. Card No:34-65 in Appendix C)

Since there are still some unreacted ZrO_2, the product was reheated at 1200 ^oC for another 5 hours. The XRD pattern of the product is given in Figure 3.5. According to Table 3.4, the main product of the reaction was found to be $Sr_7Zr(PO_4)_6$ together with a minor amount of ZrO_2.

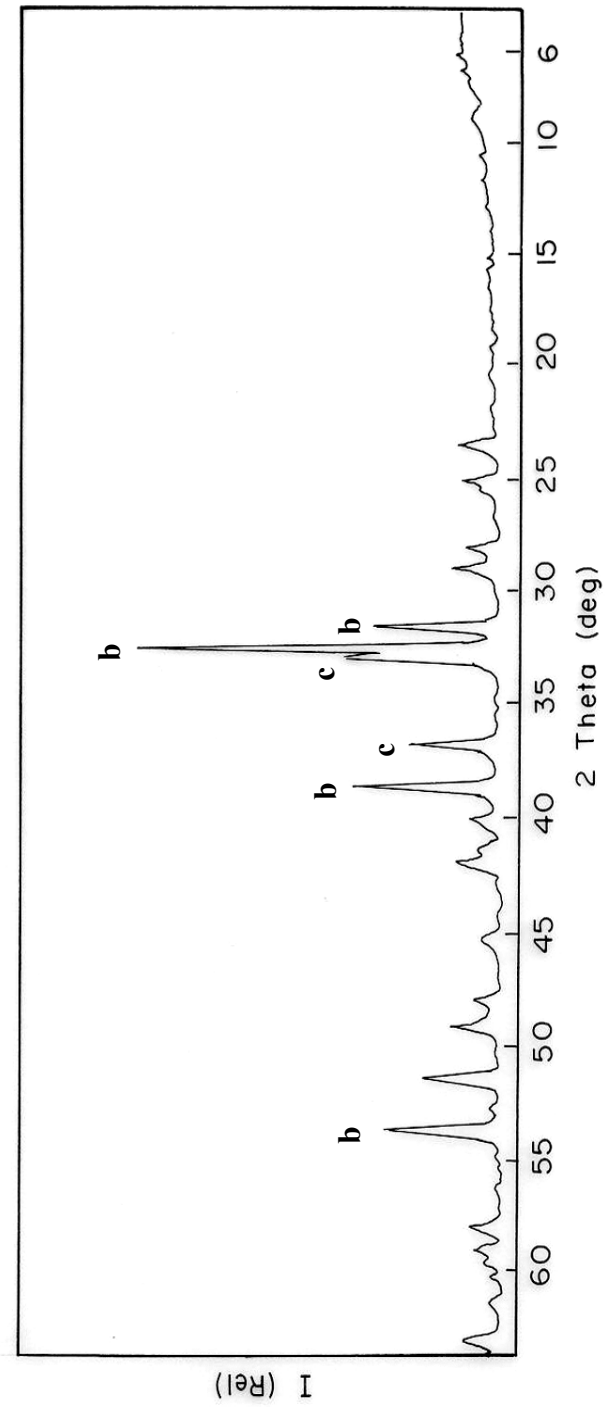

Figure 3.5 The X-ray Powder Diffraction Pattern of the Products Obtained From the Solid State Reactions of $2ZrO_2 + 2SrCO_3 + B_2O_3$ with $2(NH_4)_2HPO_4$ at 1200 ^oC (where b=$Sr_7Zr(PO_4)_6$,

Table 3.4 The X-ray Powder Diffraction Data of the Products Obtained From the S S actions $SrCO_3$ + $_3$ with $2(NH_4)_2HPO$

I/I_o	d_{obs}	Remarks
2	5.0547	**ZrO_2**
10	4.4140	**unknown**
9	4.1356	**$Sr_7Zr(PO_4)_6$**
7	3.6871	**ZrO_2**
11	3.5750	**$Sr_7Zr(PO_4)_6$**
35	3.2925	**unknown**
100	3.1940	**$Sr_7Zr(PO_4)_6$**
41	3.1516	**ZrO_2**
25	2.8320	**ZrO_2**
44	2.7048	**$Sr_7Zr(PO_4)_6$**
7	2.6171	**ZrO_2**
7	2.5063	**ZrO_2**
5	2.3243	**ZrO_2**
6	2.2050	**ZrO_2**
11	2.1544	**$Sr_7Zr(PO_4)_6$**
23	2.0641	**$Sr_7Zr(PO_4)_6$**
33	1.9853	**$Sr_7Zr(PO_4)_6$**
7	1.8434	**ZrO_2**
8	1.8122	**ZrO_2**
3	1.7468	**$Sr_7Zr(PO_4)_6$**
11	1.7071	**ZrO_2**
2	1.6915	**ZrO_2**

ZrO_2 (J.C.P.D.S. Card No: 37-1484 in Appendix B)

$Sr_7Zr(PO_4)_6$ (J.C.P.D.S. Card No:34-65 in Appendix C)

To prove that the final reaction product is mainly $Sr_7Zr(PO_4)_6$, this reference compound was tried to be synthesized by using solid state reaction. The following reaction was expected:

$$7SrCO_3(s) + ZrO_2(s) + 6(NH_4)_2HPO_4(s) \rightarrow Sr_7Zr(PO_4)_6(s) + 7CO_2(g) + 9H_2O(g)$$

The heating procedure of this reaction is given in Table 3.5.

Table 3.5. The Experimental Conditions for the Solid State Reactions of $7SrCO_3$ + ZrO_2+ $6(NH_4)_2HPO_4$

Exp.No	Temp. (^oC)	Duration (h)
Sr_7.1	300	5
Sr_7.2	800	9
Sr_7.3	1200	18

The XRD data of these products given in Table 3.6 and Table 3.7 show that at 800 ^oC the main products are α-$Sr_2P_2O_7$ (J.C.P.D.S. Card No:24-1011 in Appendix E) and α-$Sr_3(PO_4)_2$ (J.C.P.D.S. Card No:24-1008 in Appendix D), and at 1200 ^oC the main product is $Sr_7Zr(PO_4)_6$ together with a trace amount of α-$Sr_2P_2O_7$. The IR spectrum of **Exp.No:Sr_7.3** showed that monophosphate and pyrophosphate bands were present.

Table 3.6 The X-ray Powder Diffraction Data of the Products Obtained From the Solid State Reactions of $7SrCO_3$ + ZrO_2 with $6(NH_4)_2HPO_4$ at 800 ^oC

I/I_o	d_{obs}	Remarks	I/I_o	d_{obs}	Remarks
23	7.3974	**α-$Sr_2P_2O_7$**	7	2.3123	**α-$Sr_3(PO_4)_2$, α-$Sr_2P_2O_7$**
8	6.6377	**α-$Sr_3(PO_4)_2$, α-$Sr_2P_2O_7$**	12	2.2676	**α-$Sr_3(PO_4)_2$, α-$Sr_2P_2O_7$**
3	5.1547	**unknown**	8	2.2269	**α-$Sr_2P_2O_7$**
3	4.9822	**α-$Sr_2P_2O_7$**	35	2.1942	**α-$Sr_2P_2O_7$**
7	4.5483	**α-$Sr_3(PO_4)_2$**	6	2.1260	**α-$Sr_2P_2O_7$**

Table 3.6 Continued

8	4.4610	**α-$Sr_2P_2O_7$**	14	2.1081	**α-$Sr_3(PO_4)_2$**
5	3.9345	**α-$Sr_2P_2O_7$**	7	2.0830	**α-$Sr_3(PO_4)_2$**
7	3.6935	**α-$Sr_2P_2O_7$**	42	2.0419	**α-$Sr_2P_2O_7$**
58	3.4305	**α-$Sr_2P_2O_7$**	31	2.0061	**α-$Sr_3(PO_4)_2$**
80	3.4030	**α-$Sr_2P_2O_7$**	8	1.9683	**α-$Sr_2P_2O_7$**
24	3.3233	**α-$Sr_2P_2O_7$**	5	1.8911	**α-$Sr_2P_2O_7$**
24	3.1609	**ZrO_2**	11	1.8625	**α-$Sr_2P_2O_7$**
22	3.1240	**α-$Sr_2P_2O_7$**	20	1.8463	**ZrO_2**
82	3.0142	**α-$Sr_3(PO_4)_2$**	19	1.8192	**α-$Sr_3(PO_4)_2$, ZrO_2**
15	2.9767	**unknown**	14	1.7010	**α-$Sr_3(PO_4)_2$, α-$Sr_2P_2O_7$**
12	2.8358	**ZrO_2**	5	1.6809	**α-$Sr_2P_2O_7$**
100	2.6915	**α-$Sr_3(PO_4)_2$**	12	1.6682	**α-$Sr_3(PO_4)_2$, α-$Sr_2P_2O_7$**
11	2.5500	**α-$Sr_2P_2O_7$**	17	1.6101	**α-$Sr_3(PO_4)_2$, ZrO_2**
10	2.5236	**α-$Sr_2P_2O_7$**	5	1.5894	**α-$Sr_2P_2O_7$**
8	2.4050	**α-$Sr_2P_2O_7$**	13	1.5567	**α-$Sr_3(PO_4)_2$, α-$Sr_2P_2O_7$**
4	2.3639	**α-$Sr_2P_2O_7$**	6	1.5060	**α-$Sr_3(PO_4)_2$, α-$Sr_2P_2O_7$**

ZrO_2 (J.C.P.D.S. Card No: 37-1484 in Appendix B)

α-$Sr_2P_2O_7$ (J.C.P.D.S. Card No:24-1011 in Appendix E)

α-$Sr_3(PO_4)_2$ (J.C.P.D.S. Card No:24-1008 in Appendix D)

Table 3.7 The X-ray Powder Diffraction Data of the Products Obtained From the Solid State Reactions of $7SrCO_3 + ZrO_2$ with $6(NH_4)_2HPO_4$ at 1200 ^oC

I/I_o	**d_{obs}**	**Remarks**
3	7.3974	**α-$Sr_2P_2O_7$**
10	4.1519	**$Sr_7Zr(PO_4)_6$**
12	3.5932	**$Sr_7Zr(PO_4)_6$**
6	3.4360	**α-$Sr_2P_2O_7$**
4	3.4140	**α-$Sr_2P_2O_7$**
4	3.4030	**α-$Sr_2P_2O_7$**

Table 3.7 Continued

3	3.3337	**α-$Sr_2P_2O_7$**
100	3.2132	**$Sr_7Zr(PO_4)_6$**
2	3.1286	**α-$Sr_2P_2O_7$**
7	3.0185	**α-$Sr_3(PO_4)_2$**
1	2.9411	**unknown**
2	2.9005	**α-$Sr_2P_2O_7$**
49	2.7150	**$Sr_7Zr(PO_4)_6$**
4	2.1985	**α-$Sr_2P_2O_7$**
11	2.1668	**$Sr_7Zr(PO_4)_6$**
1	2.1101	**α-$Sr_3(PO_4)_2$**
20	2.0735	**$Sr_7Zr(PO_4)_6$**
5	2.0437	**α-$Sr_2P_2O_7$**
4	2.0096	**α-$Sr_3(PO_4)_2$**
36	1.9921	**$Sr_7Zr(PO_4)_6$**
4	1.8521	**$Sr_7Zr(PO_4)_6$**
3	1.8206	**α-$Sr_3(PO_4)_2$**
13	1.6490	**$Sr_7Zr(PO_4)_6$**

$Sr_7Zr(PO_4)_6$ (J.C.P.D.S. Card No:34-65 in Appendix C)

α-$Sr_2P_2O_7$ (J.C.P.D.S. Card No:24-1011 in Appendix E)

α-$Sr_3(PO_4)_2$ (J.C.P.D.S. Card No:24-1008 in Appendix D)

In boron flux reactions, excess B_2O_3 or H_3BO_3 was used as given by the following compositions and conditions in Table 2.2 (page 24).

$2ZrO_2(s) + 2SrCO_3(s) + 12B_2O_3(s) + 2(NH_4)_2HPO_4(s)$ **(Exp.No:D45)**

$2ZrO_2(s) + 2SrCO_3(s) + 12B_2O_3(s) + 2NH_4H_2PO_4(s)$ **(Exp.No:D46)**

$2ZrO_2(s) + 2SrCO_3(s) + 12H_3BO_3(s) + 2(NH_4)_2HPO_4(s)$ **(Exp.No:D47)**

$2ZrO_2(s) + 2SrCO_3(s) + 12H_3BO_3(s) + 2NH_4H_2PO_4(s)$ **(Exp.No:D48)**

In this method, four different solid state reactions were performed with **Exp.No:D45, D46, D47, D48**. The XRD data of the products at 700 ^{o}C and remarks on these reactions are given in Table 3.8. There are many phases identified in these flux reactions. For this reason, these products were reheated at 1200 ^{o}C for 5 hours. The product **(Exp.No:D45, D46)** at this temperature melted. XRD patterns of the latter two (Figure 3.6) showed that the main product is $Sr_7Zr(PO_4)_6$ with very little amount of unreacted ZrO_2 and some $Sr_3(PO_4)_2$ (J.C.P.D.S Card No:32-1251 in Appendix G) and an unknown compound (Table 3.9) instead of $ZrSr[BPO_7]$ since controlled cooling could not be established. The IR spectra related with these reactions indicated that there is monophosphate in the products.

Table 3.8. The X-ray Powder Diffraction Pattern of the Products Obtained From the Flux Reactions at 700 ^{o}C **(Exp.No:D45, D46, D47, D48)**, respectively(Only the Identified Lines Were Reported)

D45		**D46**		**D47**		**D48**		
I/I_o	**d_{obs}**	**I/I_o**	**d_{obs}**	**I/I_o**	**d_{obs}**	**I/I_o**	**d_{obs}**	**Remarks**
25	4.4897	16	4.4705	21	4.4705	24	4.4897	**$SrBPO_5$**
30	4.3589	25	4.3680	9	4.3499	7	4.3589	**$SrBPO_5$**
24	3.6615	32	3.6615	25	3.6426	27	3.6489	**BPO_4**
71	3.4250	52	3.4360	79	3.4250	82	3.4305	**$SrBPO_5$**
100	3.1656	100	3.1703	81	3.1609	81	3.1656	**ZrO_2**
14	3.0485	11	3.0355	11	30615	10	3.0615	**$SrBPO_5$**
86	2.9562	63	2.9562	100	2.9522	100	2.9603	**$SrBPO_5$**
56	2.8358	58	2.8507	59	2.8395	52	2.8432	**ZrO_2**
21	2.6234	22	2.6361	18	2.6234	20	2.6266	**ZrO_2**
18	2.5984	18	2.6109	17	2.5984	13	2.6046	**ZrO_2**
22	2.5411	19	2.5382	13	2.5411	13	2.5470	**ZrO_2**
12	2.4129	14	2.4262	14	2.4129	11	2.4156	**$SrBPO_5$**
26	2.2358	23	2.2403	31	2.2358	29	2.2403	**BPO_4**
34	2.1240	27	2.1220	32	2.1280	35	2.1320	**$SrBPO_5$**

Table 3.8 Continued

35	1.8684	29	1.8699	39	1.8729	38	1.8729	**BPO_4**
19	1.8434	21	1.8492	18	1.8478	19	1.8492	**ZrO_2**
23	1.8136	21	1.8136	22	1.8178	22	1.8178	**ZrO_2, BPO_4**
13	1.6915	13	1.6915	11	1.6951	9	1.6962	**ZrO_2**
21	1.6413	19	1.6569	20	1.6424	14	1.6524	**$Sr_7Zr(PO_4)_6$**

$SrBPO_5$ (J.C.P.D.S. Card. No:18-1270 in Appendix A)

ZrO_2 (J.C.P.D.S. Card No: 37-1484 in Appendix B)

$Sr_7Zr(PO_4)_6$ (J.C.P.D.S. Card No:34-65 in Appendix C)

BPO_4 (J.C.P.D.S. Card No:34-132 in Appendix F)

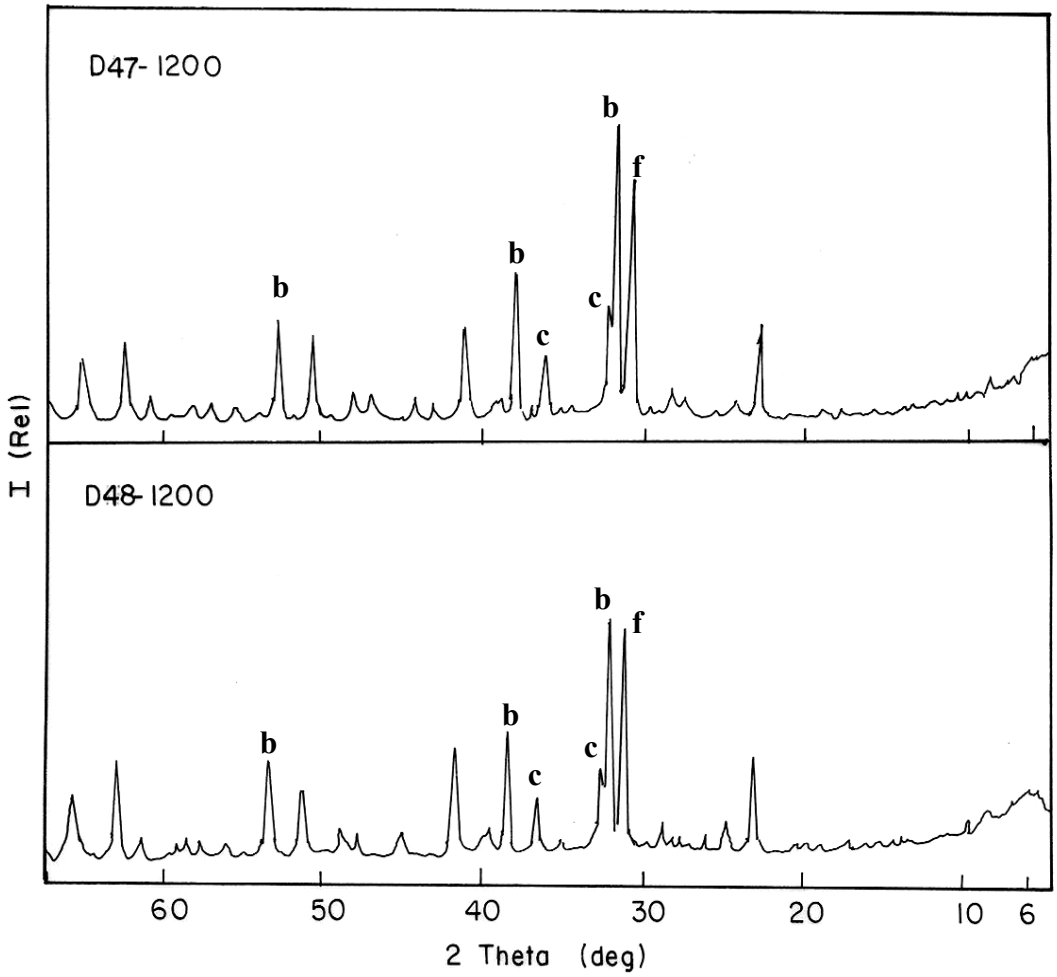

Figure 3.6 The X-ray Powder Diffraction Pattern of the Products Obtained From the Flux Reactions at 1200 ^oC **(Exp.No:D47, D48)**, respectively (where b=$Sr_7Zr(PO_4)_6$, c=ZrO_2, f= $Sr_3(PO_4)_2$)

Table 3.9 The X-ray Powder Diffraction Pattern of the Products Obtained From the Flux Reactions at 1200 ^{o}C **(Exp.No:D47, D48)**, respectively (Only the Identified Lines Were Reported)

D47		**D48**		
I/I_o	**d_{obs}**	**I/I_o**	**d_{obs}**	**Remarks**
6	7.4777	7	7.4507	**unknown**
34	4.4233	42	4.4421	**unknown**
10	3.6871	7	3.6615	**ZrO_2**
83	3.2976	97	3.3130	**$Sr_3(PO_4)_2$**
100	3.2084	100	3.2132	**$Sr_7Zr(PO_4)_6$**
37	3.1703	36	3.1797	**ZrO_2**
5	2.9603	7	2.9685	**unknown**
20	2.8395	24	2.8507	**ZrO_2**
49	2.7116	49	2.7218	**$Sr_7Zr(PO_4)_6$**
8	2.6234	11	2.6234	**ZrO_2**
5	2.5382	7	2.5500	**ZrO_2**
32	2.5120	42	2.5178	**unknown**
11	2.3366	13	2.3366	**ZrO_2**
11	2.2094	12	2.2137	**ZrO_2**
11	2.1668	15	2.1689	**$Sr_7Zr(PO_4)_6$**
27	2.0659	28	2.0716	**$Sr_7Zr(PO_4)_6$, $Sr_3(PO_4)_2$**
35	1.9887	40	1.9939	**$Sr_7Zr(PO_4)_6$, $Sr_3(PO_4)_2$**
8	1.9004	8	1.9066	**unknown**
8	1.8492	10	1.8536	**ZrO_2, $Sr_3(PO_4)_2$**
8	1.8178	8	1.8234	**ZrO_2**
10	1.7481	11	1.7545	**$Sr_7Zr(PO_4)_6$**
23	1.6479	26	1.6490	**$Sr_7Zr(PO_4)_6$, $Sr_3(PO_4)_2$**
8	1.6049	8	1.6049	**$Sr_7Zr(PO_4)_6$**
8	1.5664	8	1.5674	**$Sr_7Zr(PO_4)_6$**

ZrO_2 (J.C.P.D.S. Card No: 37-1484 in Appendix B)

$Sr_7Zr(PO_4)_6$ (J.C.P.D.S. Card No:34-65 in Appendix C)

$Sr_3(PO_4)_2$ (J.C.P.D.S. Card No:32-1251 in Appendix G)

3.1.2. Solid State Reactions of $SiO_2 + SrCO_3 + B_2O_3$ with $(NH_4)_2HPO_4$

In this study, solid state reactions were performed using the following reactants in the given proportions:

$$2SiO_2(s) + 2SrCO_3(s) + B_2O_3(s) + 2(NH_4)_2HPO_4(s) \quad \textbf{(Exp.No:D9)}$$

The reactants were heated at 900, 950 and 1100 ^oC as reported on page 24 in Table 2.3. The XRD pattern of the sample (Figure 3.7) prepared at 950 ^oC **(Exp.No:D9.2)**, the main product was found to be $SrBPO_5$ together with unreacted SiO_2 (J.C.P.D.S. Card. No:15-26 in Appendix H) and an unknown compound. In Table 3.10 $SrBPO_5$, SiO_2 and unknown lines are given. The IR spectrum of this product (Figure 3.8) showed the presence of IR modes of $SrBPO_5$ [86]. The theoretical and the experimental percent weight losses are in agreement, being 28.06 % and 33.27 %, respectively.

Then, the product was heated again at 1100 ^oC for 5 hours. The XRD pattern of the products (Figure 3.9) indicate that the main product was found to be α-$Sr_2P_2O_7$ together with very weak unknown lines. But the disappearence of $SrBPO_5$ and SiO_2 revealed the combination of these two compounds given by the following equation:

$SrBPO_5 + SiO_2 \rightarrow SrSiBPO_7$ which could be isostructural with α-$Sr_2P_2O_7$. When the radia of boron and phosphorous (r_{B3+}=0.2 Å , r_{P5+}=0.35 Å) are compared, it is impossible for B to replace P. Similarly, Si (r_{Si4+}=0.4 Å) cannot replace Sr (r_{Sr2+}=1.08 Å). It is possible for B and Si to be entered the structure as forming addition solid solution. In other word they enter into the voids of $Sr_{2-x}Si_xP_{2-y}B_yO_7$. There is no peaks of SiO_2 or $SrBPO_5$ and everything is in the solid state, the value of the x and y is nearly one. Examination of XRD pattern and indexing show some relations to $SrZrBPO_7$ structure with a=8.9243 Å ($a \approx 1/2c_{Zr}$), b=13.1548 Å ($b \approx b_{Zr}$), and c=5.4036 Å ($c \approx 1/2a_{Zr}$) in orthorhombic system.

The IR spectrum of this product showed the presence of IR modes of pyrophosphates (Figure 3.10).

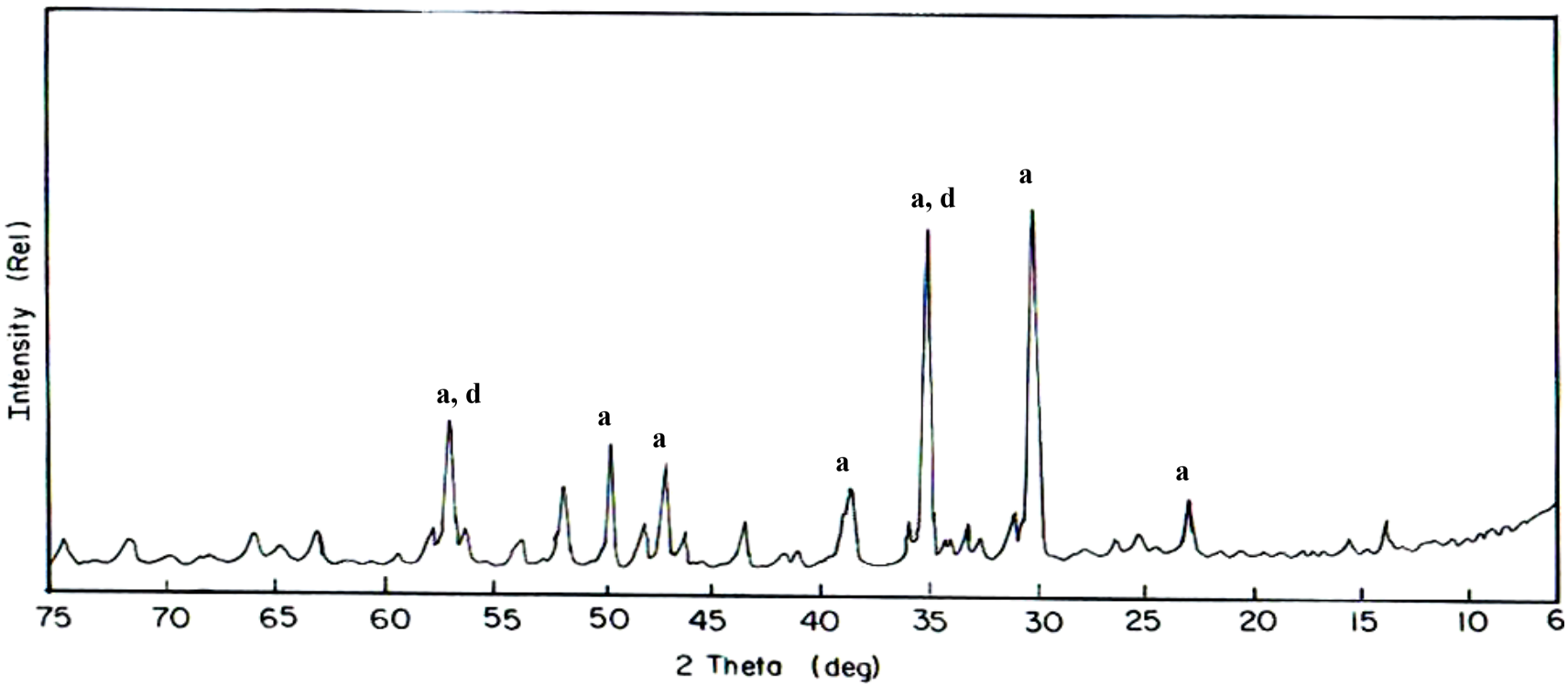

Figure 3.7 The X-ray Powder Diffraction Pattern of the Products Obtained From the Solid State Reactions of $2SiO_2 + 2SrCO_3 + B_2O_3$ with $2(NH_4)_2HPO_4$ at 950 ^oC (where a= $SrBPO_5$, d=SiO_2)

Table 3.10 The X-ray Powder Diffraction Data of the Products Obtained From the Solid State Reactions of $2SiO_2 + 2SrCO_3 + B_2O_3$ with $2(NH_4)_2HPO_4$ at 950 ^oC

I/I_o	d_{obs}	Remarks	I/I_o	d_{obs}	Remarks
2	10.0693	**unknown**	8	2.2791	**SiO_2**
8	7.4239	**unknown**	28	2.2425	**$SrBPO_5$**
4	6.6377	**unknown**	10	2.2007	**unknown**
18	4.4897	**$SrBPO_5$**	35	2.1340	**$SrBPO_5$**
5	4.0794	**unknown**	23	2.0474	**unknown**
4	3.9419	**unknown**	8	1.9818	**SiO_2**
100	3.4305	**$SrBPO_5$**	7	1.9716	**$SrBPO_5$**
14	3.3390	**unknown**	9	1.8973	**$SrBPO_5$**
7	3.2229	**unknown**	41	1.8759	**$SrBPO_5$, SiO_2**
9	3.1332	**unknown**	9	1.8521	**SiO_2**
6	3.0615	**$SrBPO_5$**	2	1.8066	**$SrBPO_5$**
5	3.0270	**unknown**	10	1.7119	**$SrBPO_5$**
94	2.9644	**$SrBPO_5$, SiO_2**	5	1.6717	**$SrBPO_5$**
9	2.9083	**unknown**	8	1.6457	**$SrBPO_5$**
22	2.7116	**$SrBPO_5$**	8	1.6435	**$SrBPO_5$**
5	2.5619	**unknown**	4	1.6007	**$SrBPO_5$**
4	2.5323	**unknown**	8	1.5330	**SiO_2**
13	2.4209	**$SrBPO_5$**	8	1.4805	**$SrBPO_5$, SiO_2**

$(2SrO).(P_2O_5).B_2O_3$ ($SrBPO_5$) (J.C.P.D.S. Card. No:18-1270 in Appendix A)

SiO_2 (J.C.P.D.S. Card. No:15-26 in Appendix H)

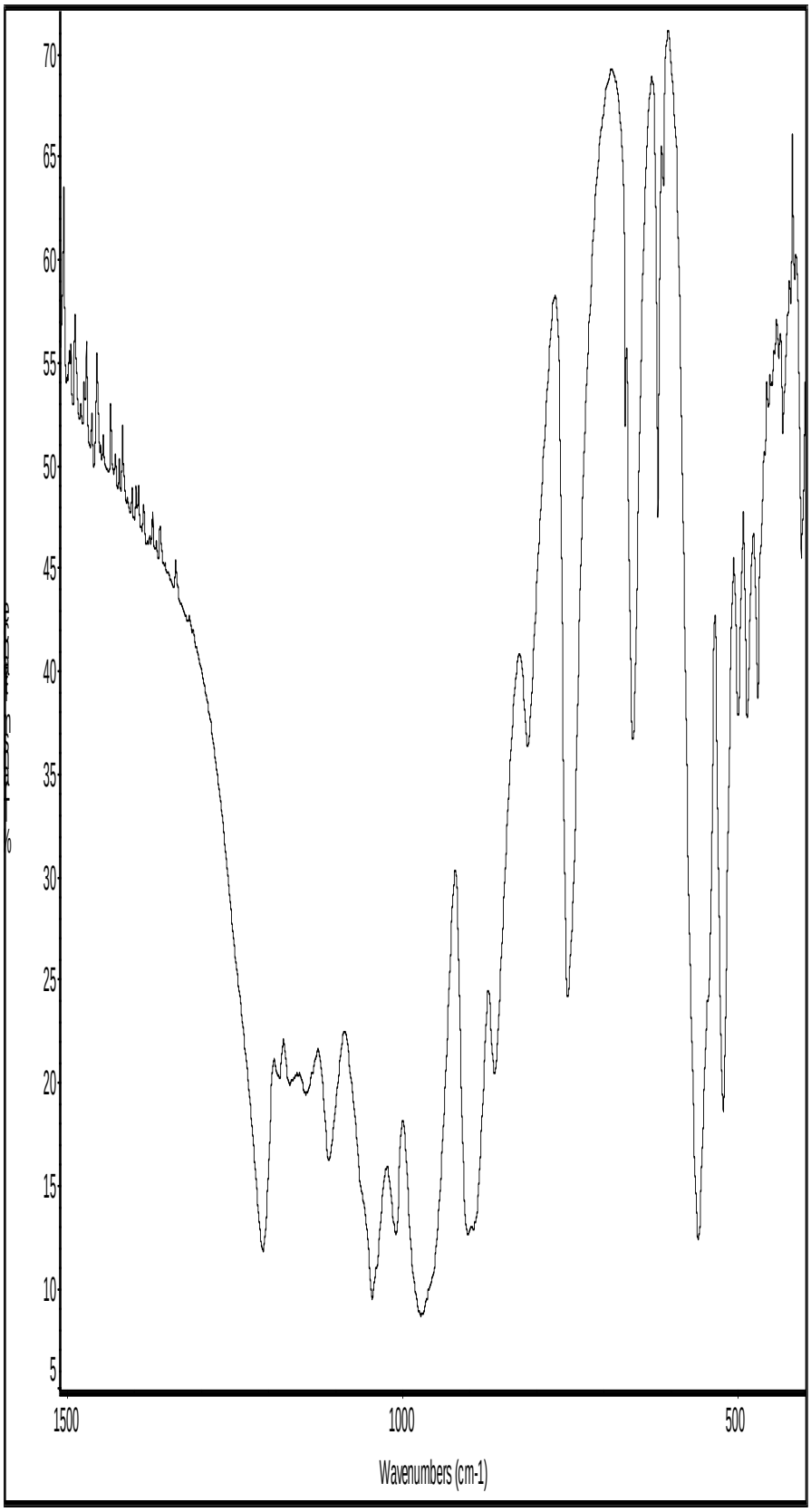

Figure 3.8 The IR Spectrum of the Products Obtained From the Solid State Reactions of $2SiO_2 + 2SrCO_3 + B_2O_3$ with $2(NH_4)_2HPO_4$ at 950 ^oC

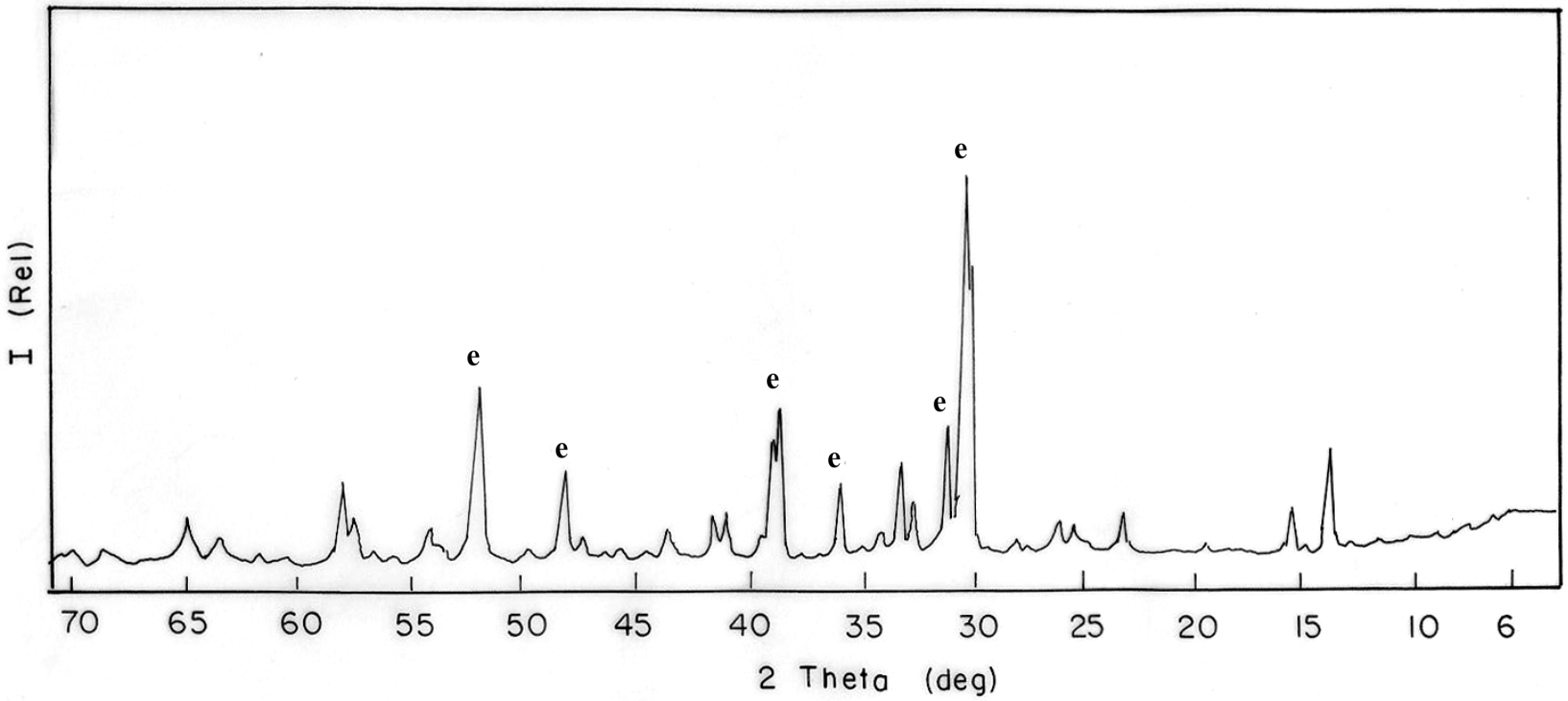

Figure 3.9 The X-ray Powder Diffraction Pattern of the Products Obtained From the Solid State

$_2 + 2SrCO_3 + B_2O_3$ with $2(NH_4)_2HPO_4$ at 1100 ^{o} α-Sr_2P

Table 3.11 The X-ray Powder Diffraction Data of the Products Obtained From the Solid State Reactions of $2SiO_2 + 2SrCO_3 + B_2O_3$ with $2(NH_4)_2HPO_4$ at 1100 ^oC

I/I_o	d_{obs}	d_{cal}	$\sin^2\theta_{obs}$	$\sin^2\theta_{cal}$	hkl	Remarks
4	13.2451	13.1548	0.00457	0.00463	010	
4	8.9341	8.9243	0.01004	0.01006	100	
29	7.3974	7.3852	0.01464	0.01469	110	**α-$Sr_2P_2O_7$**
14	6.5754	6.5774	0.01854	0.01852	020	
5	5.2855	5.29472	0.02868	0.02858	120	**α-$Sr_2P_2O_7$**
4	4.9822	4.9983	0.03228	0.03207	011	
12	4.4610	4.46215	0.04026	0.04024	200	**α-$Sr_2P_2O_7$**
10	3.9419	3.9355	0.05156	0.05173	130	**α-$Sr_2P_2O_7$**
5	3.6871	3.6926	0.05894	0.05876	220	
77	3.4360	3.4407	0.06786	0.06768	201	**α-$Sr_2P_2O_7$**
100	3.4030	3.4049	0.06919	0.06911	031	**α-$Sr_2P_2O_7$**
37	3.3285	3.3287	0.07232	0.07231	211	**α-$Sr_2P_2O_7$**
16	3.1797	3.1812	0.07924	0.07917	131	
28	3.1240	3.1276	0.08210	0.08191	230	**α-$Sr_2P_2O_7$**
11	3.0485	3.0487	0.08621	0.08620	221	**α-$Sr_2P_2O_7$**
4	2.9891	2.9748	0.08967	0.09054	300	
21	2.8966	2.9015	0.09549	0.09517	310	**α-$Sr_2P_2O_7$**
2	2.7955	2.8093	0.10253	0.10152	041	
41	2.7015	2.7069	0.10978	0.10935	231	**α-$Sr_2P_2O_7$**
32	2.6815	2.6797	0.11143	0.11158	141	**α-$Sr_2P_2O_7$**
8	2.6457	2.6466	0.11447	0.11439	012	**α-$Sr_2P_2O_7$**
14	2.5500	2.5563	0.12322	0.12261	311	**α-$Sr_2P_2O_7$**
12	2.5236	2.5373	0.12581	0.12445	112	**α-$Sr_2P_2O_7$**
9	2.4050	2.4066	0.13852	0.13834	122	**α-$Sr_2P_2O_7$**
4	2.3690	2.3774	0.14276	0.14176	241	**α-$Sr_2P_2O_7$**
5	2.3075	2.3002	0.15048	0.15143	032	**α-$Sr_2P_2O_7$**
4	2.2768	2.2763	0.15456	0.15463	212	**α-$Sr_2P_2O_7$**
3	2.2425	2.2402	0.15932	0.15965	331	**α-$Sr_2P_2O_7$**
8	2.2291	2.2274	0.16124	0.16149	132	**α-$Sr_2P_2O_7$**

Table 3.11 Contiuned

25	2.1964	2.1997	0.16608	0.16559	410	**α-$Sr_2P_2O_7$**
48	2.0419	2.0425	0.19217	0.19206	341	**α-$Sr_2P_2O_7$**
7	1.9767	1.9773	0.20505	0.20493	312	**α-$Sr_2P_2O_7$**
11	1.9649	1.9678	0.20752	0.20692	421	**α-$Sr_2P_2O_7$**
4	1.9129	1.9135	0.21896	0.21882	322	**α-$Sr_2P_2O_7$**
5	1.8911	1.8909	0.22403	0.22408	242	**α-$Sr_2P_2O_7$**
14	1.8639	1.8661	0.23061	0.23007	431	**α-$Sr_2P_2O_7$**
22	1.8492	1.8463	0.23430	0.23504	440	**α-$Sr_2P_2O_7$**
2	1.7532	1.7499	0.26065	0.26165	113	
5	1.7443	1.7471	0.26334	0.26248	441	**α-$Sr_2P_2O_7$**
8	1.7034	1.7052	0.27612	0.27554	123	**α-$Sr_2P_2O_7$**
5	1.6774	1.6703	0.28474	0.28720	203	**α-$Sr_2P_2O_7$**
12	1.6659	1.6661	0.28869	0.28863	033	**α-$Sr_2P_2O_7$**
6	1.5894	1.5798	0.31716	0.32104	043	**α-$Sr_2P_2O_7$**
5	1.5606	1.5609	0.32899	0.32887	233	**α-$Sr_2P_2O_7$**

α-$Sr_2P_2O_7$ (J.C.P.D.S. Card No:24-1011 in Appendix E)

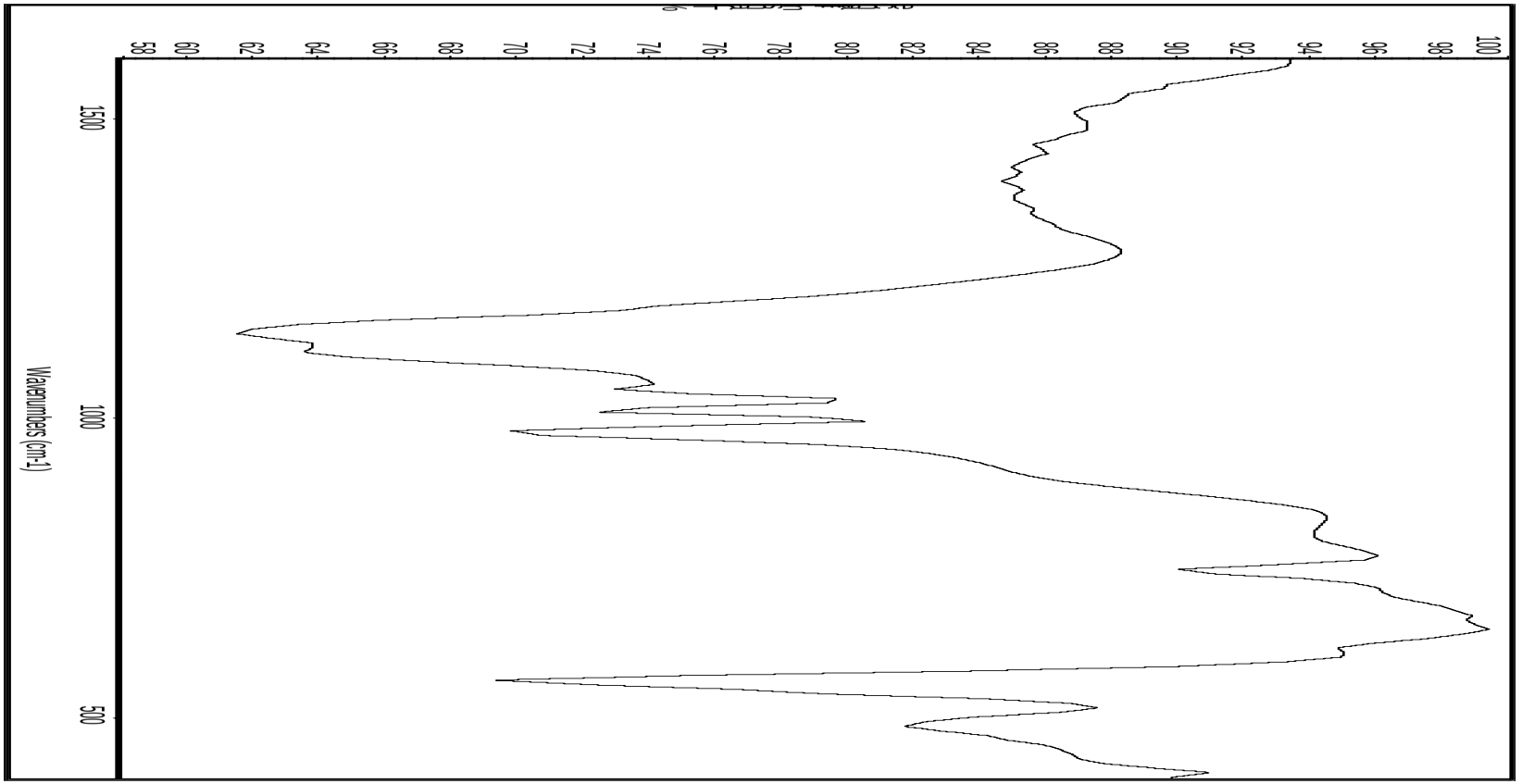

Figure 3.10 The IR Spectrum of the Products Obtained From the Solid State Reactions of $2SiO_2$ + $2SrCO_3$ + B_2O_3 with $2(NH_4)_2HPO_4$ at 1100 ^oC

3.1.3. Solid State Reactions of $2ZrO_2 + 2CaCO_3 + B_2O_3$ with $2(NH_4)_2HPO_4$

In this part of the study, Zr and Ca containing borophosphate compounds were attempted to be synthesized using solid state reactions.

The following compositions were used:

a) $2ZrO_2(s) + 2CaCO_3(s) + B_2O_3(s) + 2(NH_4)_2HPO_4(s)$ **(Exp.No:D2)**

b) $2ZrO_2(s) + 2CaCO_3(s) + B_2O_3(s) + 4(NH_4)_2HPO_4(s)$ **(Exp.No:D3)**

In the first method, ZrO_2 and B_2O_3 remained unreacted when the mixture was heated at 900 ^oC **(Exp.No:D2)** for 12h as given in Table 2.4 (page 25). α-$CaZr(PO_4)_2$ (J.C.P.D.S. Card No:30-293 in Appendix I) was found to be minor product with unreacted ZrO_2 at 950 ^oC **(Exp.No:D2A)** for 14 more hours heating time. At 1200 ^oC **(Exp.No:D2B)**, weak lines of α-$CaZr(PO_4)_2$ together with unreacted ZrO_2 and an unknown compound were observed (Table 3.12).

Table 3.12 The X-ray Powder Diffraction Data of the Products Obtained From the Solid State Reactions of 2ZrO + $2CaCO_3$ + B $_3$ with $2(NH_4)_2HPO_4$ at 1200 ^oC

I/I_o	d_{obs}	Remarks	I/I_o	d_{obs}	Remarks
20	6.5125	**unknown**	13	2.1900	**ZrO_2**
20	6.4718	**unknown**	15	2.0220	**ZrO_2**
23	3.6364	**ZrO_2**	11	1.9921	**ZrO_2**
30	3.1988	**unknown**	20	1.8478	**ZrO_2**
100	3.1609	**ZrO_2**	24	1.8178	**ZrO_2**
48	2.8735	**unknown**	9	1.7821	**ZrO_2**
63	2.8395	**ZrO_2**	13	1.6951	**ZrO_2**
20	2.6234	**ZrO_2**	14	1.6546	**ZrO_2**
43	2.5984	**ZrO_2**	8	1.6101	**ZrO_2**
18	2.5411	**ZrO_2**	9	1.5000	**ZrO_2**

ZrO_2 (J.C.P.D.S. Card No: 37-1484 in Appendix B)

In the second part, the same experiment was performed with excess phosphating agent. In the first heat treatment at 900 ^{o}C **(Exp.No:D3)** for 12 h., unreacted ZrO_2 was present in the XRD pattern. When the product was reheated at 950 ^{o}C **(Exp.No:D3A)** for 14 hours, $CaZr(BO_3)_2$ (J.C.P.D.S. Card No:24-349 in Appendix J) was found to be the major compound. As seen in Table 3.13 two side products, $CaZr_4(PO_4)_6$ (J.C.P.D.S. Card No:33-321 in Appendix K) and $CaZr(PO_4)_2$ were present in the final reaction heated at 1200 ^{o}C **(Exp.No:D3B)** for 6 hours.

Table 3.13 The X-ray Powder Diffraction Data of the Products obtained from the Solid State Reactions of $2ZrO_2 + 2CaCO_3 + B_2O_3$ with $4(NH_4)_2HPO_4$ at 1200 ^{o}C

I/I_o	d_{obs}	Remarks	I/I_o	d_{obs}	Remarks
22	6.4921	**unknown**	54	2.8507	**unknown**
25	6.3527	**unknown**	49	2.8395	**$CaZr_4(PO_4)_6$**
52	4.5582	**$CaZr_4(PO_4)_6$**	35	2.5411	**$CaZr_4(PO_4)_6$**
76	4.3955	**$CaZr_4(PO_4)_6$**	22	2.0220	**$CaZr_4(PO_4)_6$**
21	4.0715	**unknown**	13	1.9784	**$CaZr_4(PO_4)_6$**
72	3.8067	**$CaZr_4(PO_4)_6$**	18	1.9004	**$CaZr_4(PO_4)_6$**
26	3.6177	**$CaZr(PO_4)_2$**	15	1.7821	**$CaZr_4(PO_4)_6$**
24	3.3600	**$CaZr(PO_4)_2$**	12	1.7010	**$CaZr_4(PO_4)_6$**
88	3.1656	**$CaZr_4(PO_4)_6$**	22	1.6614	**$CaZr_4(PO_4)_6$**
100	2.8697	**$CaZr_4(PO_4)_6$**			

$CaZr_4(PO_4)_6$ (J.C.P.D.S. Card No:33-321 in Appendix K)

$CaZr(PO_4)_2$ (J.C.P.D.S. Card No: 33-320 in Appendix L)

3.1.4. Solid State Reactions of $2Al_2O_3 + B_2O_3$ with $2(NH_4)_2HPO_4$

The solid state reaction between Al_2O_3, B_2O_3, and $(NH_4)_2HPO_4$ in a 2:1:2 molar ratio was performed at 900 ^{o}C, 950 ^{o}C and 1100 ^{o}C. At all temperatures, $AlPO_4$ (J.C.P.D.S. Card No: 11-500 in Appendix M) was obtained. At 1100 ^{o}C, minor product was $Al_5(BO_3)O_6$ (J.C.P.D.S. Card No:34-1039 in Appendix N). The IR data showed the presence of BO_3 and PO_4 modes at 1235, 758, 707 and 1122, 567, 488 cm^{-1}, respectively.

Table 3.14 The X-ray Powder Diffraction Data of the Products Obtained From the Solid State Reactions of $2Al_2O_3 + B_2O_3$ with $2(NH_4)_2HPO_4$ at 1100 ^oC with **Exp.No:D1.3**

I/I_o	d_{obs}	Remarks	I/I_o	d_{obs}	Remarks
5	5.3679	**$Al_5(BO_3)O_6$**	16	2.5091	**$AlPO_4$**
4	4.3589	**$Al_5(BO_3)O_6$**	2	2.1380	**$AlPO_4$**
100	4.0794	**$AlPO_4$**	2	2.0382	**$AlPO_4$**
2	3.5451	**$AlPO_4$**	5	1.9483	**$Al_5(BO_3)O_6$**
2	3.3814	**$Al_5(BO_3)O_6$**	5	1.8881	**$AlPO_4$**
11	3.1656	**$AlPO_4$**	2	1.7058	**$AlPO_4$**
14	2.8697	**$AlPO_4$**	3	1.6250	**$AlPO_4$**
2	2.6881	**$Al_5(BO_3)O_6$**			

$AlPO_4$ (J.C.P.D.S. Card No:11-500 in Appendix M)
$Al_5(BO_3)O_6$ (J.C.P.D.S. Card No:34-1039 in Appendix N)

3.1.5. Solid State Reactions of H_3BO_3 and B_2O_3 with $(NH_4)_2HPO_4$

In this study, $B_2[BPO_7]$ was tried to be synthesized using two different reactant groups given by the following compositions:

a) $3B_2O_3(s) + 2(NH_4)_2HPO_4(s)$ **(Exp.No:K1)**
b) $3H_3BO_3(s) + (NH_4)_2HPO_4(s)$ **(Exp.No:B3)**

The XRD data of these compounds are given in Table 3.15., Table 3.16., respectively. In the first case **(Exp.No:K1)**, BPO_4 (J.C.P.D.S. Card No:34-132 in Appendix F) was obtained together with H_3BO_3 which is obtained through the absorption of water by unreacted B_2O_3.

Table 3.15 The X-ray Powder Diffraction Data of the Products Obtained From the Solid State Reactions of $3B_2O_3$ with $2(NH_4)_2HPO_4$ at 800, 950 ^oC (Only the Identified Lines Were Reported)

K1			**K2**		
I/I_o	**d_{obs}**	**Remarks**	**I/I_o**	**d_{obs}**	**Remarks**
16	6.0207	**H_3BO_3**	7	6.0558	**unknown**
100	3.6489	**BPO_4**	100	3.6489	**BPO_4**
23	3.2278	**H_3BO_3**	11	3.2084	**H_3BO_3**
22	3.2084	**H_3BO_3**	5	3.0791	**BPO_4**
35	2.2630	**BPO_4**	38	2.2584	**BPO_4**
11	1.8669	**H_3BO_3**	11	1.8654	**BPO_4**
11	1.8639	**BPO_4**	5	1.8220	**BPO_4**

BPO_4 (J.C.P.D.S. Card No:34-132 in Appendix F)

H_3BO_3 (J.C.P.D.S. Card No:30-199 in Appendix O)

In the second method, again BPO_4 and H_3BO_3 were obtained instead of a new product. The product of **Exp.No:B3** were reheated at 1100 ^oC and glassy phase was observed.

Table 3.16 The X-ray Powder Diffraction Data of the Products Obtained From the Solid State Reactions of $3H_3BO_3$ with $(NH_4)_2HPO_4$ at 900, 1000 ^oC (Only the Identified Lines Were Reported)

B3.1			**B3.2**		
I/I_o	**d_{obs}**	**Remarks**	**I/I_o**	**d_{obs}**	**Remarks**
6	6.0558	**unknown**	12	6.0032	**H_3BO_3**
7	5.9345	**H_3BO_3**	14	5.9176	**H_3BO_3**
100	3.6301	**BPO_4**	4	4.9822	**H_3BO_3**
4	3.3182	**H_3BO_3**	4	4.0636	**H_3BO_3**
14	3.1845	**H_3BO_3**	4	3.7261	**unknown**
6	3.0659	**BPO_4**	100	3.6301	**BPO_4**
3	3.0058	**unknown**	4	3.5157	**H_3BO_3**
26	2.2538	**BPO_4**	5	3.3285	**BPO_4**

Table 3.16 Continued

2	1.9716	**BPO_4**	17	3.1845	**H_3BO_3**
9	1.8610	**BPO_4**	6	3.0659	**BPO_4**
3	1.8178	**BPO_4**	4	2.7218	**H_3BO_3**
			32	2.2493	**H_3BO_3**
			4	2.0149	**H_3BO_3**
			4	1.9700	**BPO_4**
			4	1.8150	**BPO_4**

BPO_4 (J.C.P.D.S. Card No:34-132 in Appendix F)

H_3BO_3 (J.C.P.D.S. Card No:30-199 in Appendix O)

3.1.6. Solid State Reactions of ZrO_2+Na_2CO_3+H_3BO_3 with $NH_4H_2PO_4$

In this work, the solid state reactions of the following composition was investigated at 910 ^oC for 5.5 hours:

$ZrO_2(s) + Na_2CO_3(s) + H_3BO_3(s) + NH_4H_2PO_4(s)$ **(Exp.No:D53)**

The XRD data are given in Table 3.17. In the pattern unreacted ZrO_2 was the major compound together with $Na_2Zr(PO_4)_6$ (J.C.P.D.S. Card No:35-125 in Appendix P) and $Na_{5-4x}Zr_{1+x}(PO_4)_3$ (J.C.P.D.S. Card No:37-384 in Appendix R).

Table 3.17 The X-ray Powder Diffraction Data of the Products Obtained From the Solid State Reactions of ZrO_2+Na_2CO_3+H_3BO_3 with $NH_4H_2PO_4$ at 910 ^oC

I/I_o	**d_{obs}**	**Remarks**
10	7.4501	**unknown**
17	7.2419	**$Na_2Zr(PO_4)_6$, $Na_{5-4x}Zr_{1+x}(PO_4)_3$**
36	4.5681	**$Na_{5-4x}Zr_{1+x}(PO_4)_3$**
34	4.4233	**$Na_{5-4x}Zr_{1+x}(PO_4)_3$**
9	4.0248	**$Na_{5-4x}Zr_{1+x}(PO_4)_3$**

Table 3.17 Continued

40	3.8204	**unknown**
100	3.1609	**ZrO_2**
77	2.8811	**$Na_2Zr(PO_4)_6$, $Na_{5-4x}Zr_{1+x}(PO_4)_3$**
78	2.8395	**ZrO_2**
41	2.6297	**ZrO_2**
24	2.5441	**ZrO_2**
5	2.2861	**ZrO_2**
14	2.2115	**ZrO_2**
10	2.0167	**ZrO_2**
16	1.9401	**$Na_2Zr(PO_4)_6$**
16	1.8463	**ZrO_2**
23	1.8150	**ZrO_2**
16	1.8025	**ZrO_2**
12	1.6740	**ZrO_2**

$Na_2Zr(PO_4)_6$ (J.C.P.D.S. Card No: 35-125 in Appendix P)

$Na_{5-4x}Zr_{1+x}(PO_4)_3$ (J.C.P.D.S. Card No: 37-384 in Appendix R)

3.2. Hydrothermal Reactions

3.2.1. Hydrothermal Reactions of $ZrO_2 + SrCO_3 + H_3BO_3 + (NH_4)_2HPO_4$

In this section, hydrothermal reaction of the solution composed of ZrO_2 + $SrCO_3$ + H_3BO_3 + $(NH_4)_2HPO_4$ **(Exp.No:HT)** was performed as explained in Section 2.3.2 (page 27). The temperature was kept at 150 ^oC for 12 days. The product was an unidentified compound with a highest d-spacing of 7.53 Å and BPO_4 (Table 3.18). The presence of weak OH peak in IR spectra (Figure 3.11 at Room Temperature) revealed that the formation of small amount of hydroxyl compound. The peaks

related with crystalline water and hydrogen bonding were also identified at 3500-3200 and 1600 cm^{-1}.

Table 3.18 The X-ray Diffraction Data of the Products Obtained From the Hydrothermal Reactions of $ZrO_2 + SrCO_3 + H_3BO_3 + (NH_4)_2HPO_4$ at 150 ^oC for 12 days with **Exp.No:HT**

I/I_o	d_{obs}	Remarks	I/I_o	d_{obs}	Remarks
14	16.4196	**unidentified**	20	3.8981	**unidentified**
8	13.5061	**unidentified**	75	3.6300	**BPO_4**
10	12.8319	**unidentified**	12	3.4360	**unidentified**
7	10.6970	**unidentified**	9	3.3130	**unidentified**
11	8.0301	**unidentified**	7	3.1845	**$H_2ZrP_2O_8$, α-$Zr(HPO_4)_2$**
100	7.5300	**$H_2ZrP_2O_8$, α-$Zr(HPO_4)_2$**	8	3.0659	**unidentified**
7	6.6591	**unidentified**	5	2.8811	**unidentified**
7	6.2007	**unidentified**	36	2.6457	**unidentified**
10	5.6750	**unidentified**	31	2.6329	**α-$Zr(HPO_4)_2$**
4	5.5686	**unidentified**	6	2.4129	**α-$Zr(HPO_4)_2$**
6	5.3398	**unidentified**	38	2.2584	**BPO_4, $H_2ZrP_2O_8$**
8	5.1803	**unidentified**	11	2.1140	**unidentified**
7	4.9118	**$H_2ZrP_2O_8$**	8	2.0511	**$H_2ZrP_2O_8$, α-$Zr(HPO_4)_2$**
7	4.7989	**unidentified**	7	2.0025	**α-$Zr(HPO_4)_2$**
36	4.5100	**$H_2ZrP_2O_8$**	8	1.8774	**unidentified**
28	4.4327	**unidentified**	20	1.8625	**BPO_4, $H_2ZrP_2O_8$**
14	4.1850	**unidentified**	7	1.8150	**BPO_4, $H_2ZrP_2O_8$**
16	4.0402	**unidentified**	5	1.7662	**unidentified**

$H_2ZrP_2O_8$ (J.C.P.D.S. Card. No:21-395 in Appendix T)

α-$Zr(HPO_4)_2$ (J.C.P.D.S. Card. No:31-1486 in Appendix U)

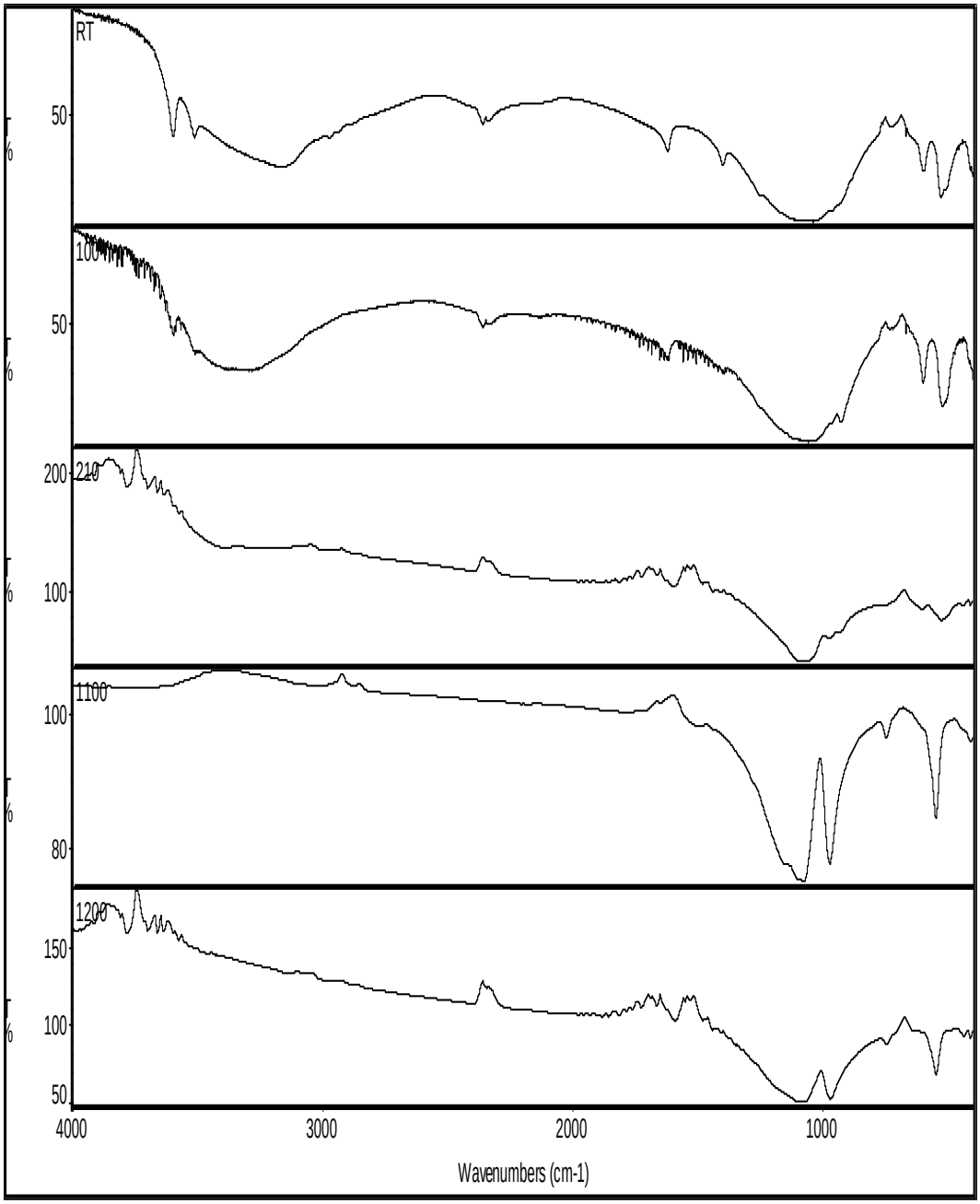

Figure 3.11 The IR Spectra of the Products Obtained From the Reactions of ZrO_2 + $SrCO_3$ + H_3BO_3 + $(NH_4)_2HPO_4$ After Filtering at Room Temperature, 100 ^oC, 210 ^oC, 1100 ^oC, 1200 ^oC, respectively

The DTA data (Figure 3.12) showed an endothermic peak at 201.81 ^oC corresponding to the decomposition of weak hydroxyl group. The peak around 1132 ^oC corresponds to the phase transition and a broad peak around 1200-1550 ^oC corresponds to melting.

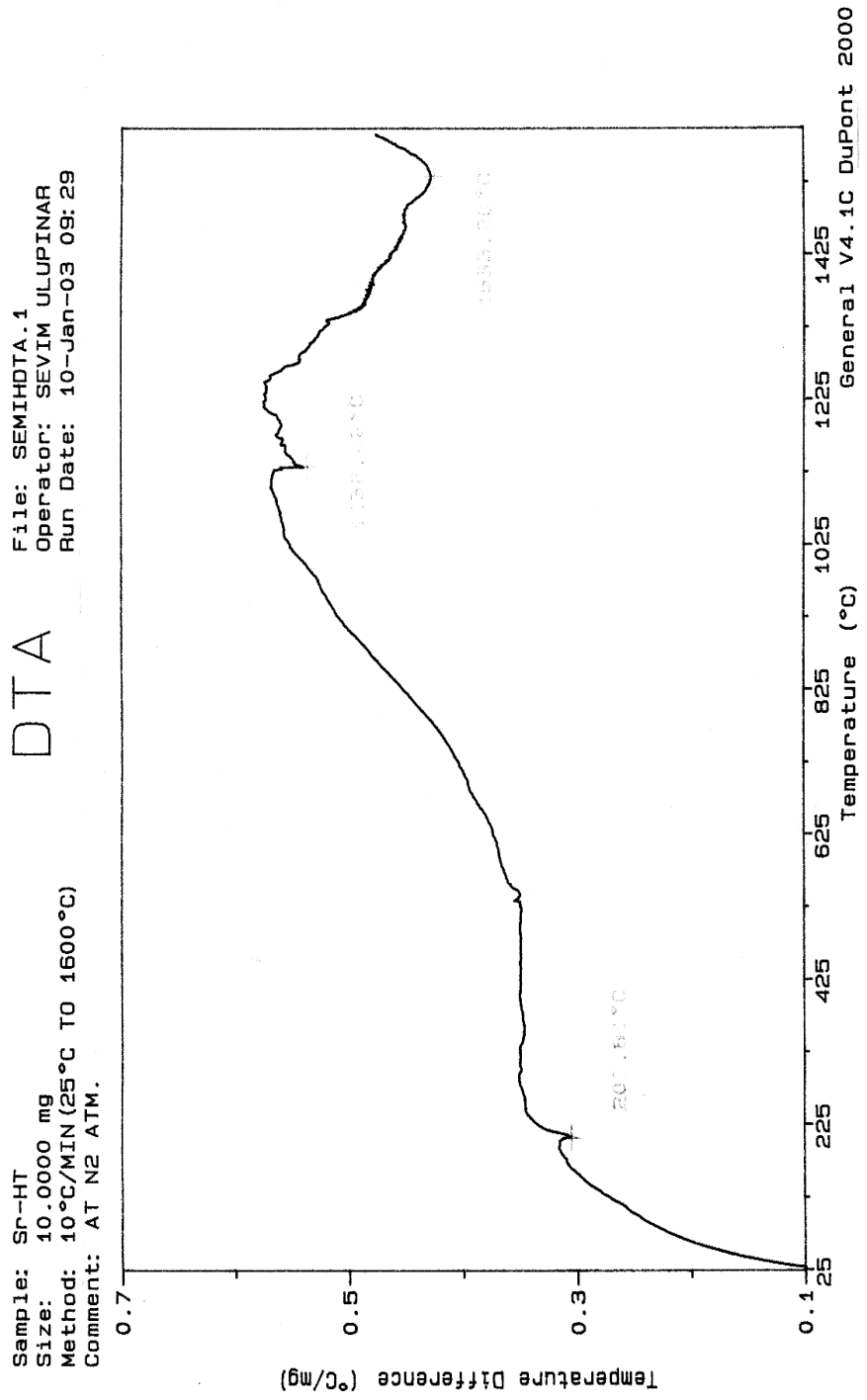

Figure 3.12 DTA Analysis of the Products Obtained From the Hydrothermal Reactions of $ZrO_2 + SrCO_3 + H_3BO_3 + (NH_4)_2HPO_4$ after filtering

For this reason, products were heated at 210 ^oC, 1100 ^oC, and 1200 ^oC. The heating procedure of this treatment is given in Table 3.19.

Table 3.19 The Experimental Conditions for the Solid State Reactions of the Products Obtained From the Hydrothermal Reactions of ZrO_2 + $SrCO_3$ + H_3BO_3 + $(NH_4)_2HPO_4$

Exp.No	**Temp. (^oC)**	**Duration (h)**
HT-210	210	10
HT-1100	1100	5
HT-1200	1200	13

The XRD data of the products are given in Table 3.20

Table 3.20 XRD Data of the Products Heated at 1100 ^oC, 1200 ^oC Obtained From the Hydrothermal Reaction of ZrO_2 + $SrCO_3$ + H_3BO_3 + $(NH_4)_2HPO_4$, respectively

HT-1100		**HT-1200**		
I/I_o	**d_{obs}**	**I/I_o**	**d_{obs}**	**Remarks**
30	4.7552	32	4.7552	**ZrP_2O_7**
-	-	8	4.6288	
-	-	11	4.3589	
100	4.1194	100	4.1194	**ZrP_2O_7**
-	-	10	3.8067	
38	3.6807	32	3.6871	**ZrP_2O_7**
14	3.6364	-	-	**BPO_4**
32	3.3654	31	3.3654	**ZrP_2O_7**
2	3.2180	2	3.2084	**ZrP_2O_7**
2	3.1424	5	3.1424	**ZrP_2O_7**
2	3.0442	-	-	**ZrP_2O_7**
2	2.9849	-	-	**ZrP_2O_7**
31	2.9162	34	2.9123	**ZrP_2O_7**
38	2.4864	34	2.4864	**ZrP_2O_7**
7	2.3792	6	2.3792	**ZrP_2O_7**
5	2.2861	4	2.2908	**ZrP_2O_7**

Table 3.20 Continued

5	2.2516	-	-	**BPO_4**
5	2.0603	3	2.0641	**ZrP_2O_7**
4	2.0008	5	1.9991	**ZrP_2O_7**
3	1.9410	3	1.9450	**ZrP_2O_7**
11	1.8911	11	1.8911	**ZrP_2O_7**
22	1.8434	16	1.8434	**ZrP_2O_7**
3	1.7984	3	1.7997	**ZrP_2O_7**
15	1.6821	10	1.6821	**ZrP_2O_7**
19	1.5843	15	1.5864	**ZrP_2O_7**

ZrP_2O_7 (J.C.P.D.S. Card. No:24-1490 in Appendix S)

According to Table 3.20, ZrP_2O_7 (J.C.P.D.S. Card. No:24-1490) was the main product. This proved that the initial product was $Zr(HPO_4)_2.xH_2O$ resembling J.C.P.D.S. Card. No:21-325 (in Appendix T) or 31-1486 (in Appendix U). At 210 ^oC, ZrP_2O_7 formation happened but BPO_4 and $Zr(HPO_4)_2$ with the highest peak at 7.53 Å were still present. At 1100 ^oC and 1200 ^oC, pure ZrP_2O_7 was obtained. In EDX data no strontium peaks was seen. So it was decided that Sr was not in the product but remained in the solution after filtering. For this reason, $Sr_2Zr(P_2O_7)_2$ was tried to synthesize through solid state reactions. The experimental conditions are given in Table 3.21.

Table 3.21 The Experimental Conditions for the Solid State Reactions of the Products Obtained From the Reactions of $2SrCO_3+ZrO_2$ with $4(NH_4)_2HPO_4$

Exp.No	**Temp. (^oC)**	**Duration (h)**
Sr_2-1000	1000	10
Sr_2-1100	1100	4
Sr_2-1200	1200	5.5

The XRD data of these reactions were given in Table 3.22. According to the Table 3.22, α-$Sr_2P_2O_7$ and ZrP_2O_7 were obtained as different phases and did not form a solid solution.

Table 3.22 The X-ray Powder Diffraction Data of the Products Obtained From the Solid State Reactions of $2SrCO_3+ZrO_2$ with $4(NH_4)_2HPO_4$ at 1000 ^oC, 1100 ^oC, 1200 ^oC, respectively (Only the Identified Lines Were Reported)

Sr_2-1000		**Sr_2-1100**		**Sr_2-1200**		
I/I_o	**d_{obs}**	**I/I_o**	**d_{obs}**	**I/I_o**	**d_{obs}**	**Remarks**
20	7.3974	24	7.3710	25	7.3974	**α-$Sr_2P_2O_7$**
7	6.5954	8	6.5954	11	6.5537	**α-$Sr_2P_2O_7$**
30	4.7552	29	4.7552	31	4.7552	**ZrP_2O_7**
7	4.4515	8	4.4515	10	4.4610	**α-$Sr_2P_2O_7$**
100	4.1194	100	4.1194	100	4.1113	**ZrP_2O_7**
8	3.9419	6	3.9345	10	3.9345	**α-$Sr_2P_2O_7$**
41	3.6807	33	3.6807	35	3.6807	**ZrP_2O_7**
44	3.4360	57	3.4360	55	3.4305	**α-$Sr_2P_2O_7$**
80	3.3976	84	3.4030	76	3.4030	**α-$Sr_2P_2O_7$**
48	3.3654	38	3.3600	40	3.3600	**ZrP_2O_7**
23	3.3390	31	3.3285	31	3.3285	**α-$Sr_2P_2O_7$**
51	3.1940	15	3.1797	19	3.1750	**α-$Sr_2P_2O_7$**
13	3.1240	18	3.1240	30	3.1240	**α-$Sr_2P_2O_7$**
34	2.9044	39	2.9005	46	2.9005	**α-$Sr_2P_2O_7$**
32	2.7015	39	2.7015	40	2.6981	**α-$Sr_2P_2O_7$**
28	2.6749	25	2.6815	32	2.6815	**α-$Sr_2P_2O_7$**
8	2.5559	11	2.5529	13	2.5559	**α-$Sr_2P_2O_7$**
9	2.5265	13	2.5236	15	2.5236	**α-$Sr_2P_2O_7$**
43	2.4836	34	2.4808	36	2.4808	**ZrP_2O_7**
7	2.4156	9	2.4050	9	2.4077	**α-$Sr_2P_2O_7$**
7	2.3741	7	2.3792	8	2.3766	**ZrP_2O_7**
13	2.2861	5	2.2815	7	2.2791	**ZrP_2O_7**
4	2.2291	7	2.2269	9	2.2269	**α-$Sr_2P_2O_7$**
17	2.1964	24	2.1942	21	2.1942	**α-$Sr_2P_2O_7$**
4	2.1300	4	2.1300	6	2.1300	**α-$Sr_2P_2O_7$**
41	2.0437	46	2.0437	58	2.0419	**α-$Sr_2P_2O_7$**
8	1.9683	11	1.9683	14	1.9666	**α-$Sr_2P_2O_7$**

Table 3.22 Continued

15	1.8896	12	1.8896	16	1.8881	**α-$Sr_2P_2O_7$**
11	1.8654	9	1.8639	15	1.8639	**α-$Sr_2P_2O_7$**
30	1.8434	29	1.8434	31	1.8449	**ZrP_2O_7**
7	1.6986	8	1.7010	10	1.7034	**α-$Sr_2P_2O_7$**
20	1.5864	16	1.5843	19	1.5843	**ZrP_2O_7**
5	1.5321	4	1.5302	4	1.5293	**ZrP_2O_7**

According to Ray et al [42], the group IV elements titanium, zirconium and tin, together with cerium and thorium in their highest oxidation states form phosphates with the general formula $M(HPO_4)_2.xH_2O$, all of them are polymers with a layer structure (Figure 3.13). Each layer consists of an array of nearly coplanar, six-coordinate, group IV elements linked through tetrahedral PO_4 groups lying alternately above and below the plane; each group IV element is connected to six oxygen atoms belonging to six different phosphate groups, so that the polymer network has a connectivity that is partly four and partly six. The layers are joined together by very long hydrogen bonds between the non-bonding oxygens of the phosphate tetrahedra in adjacent layers.

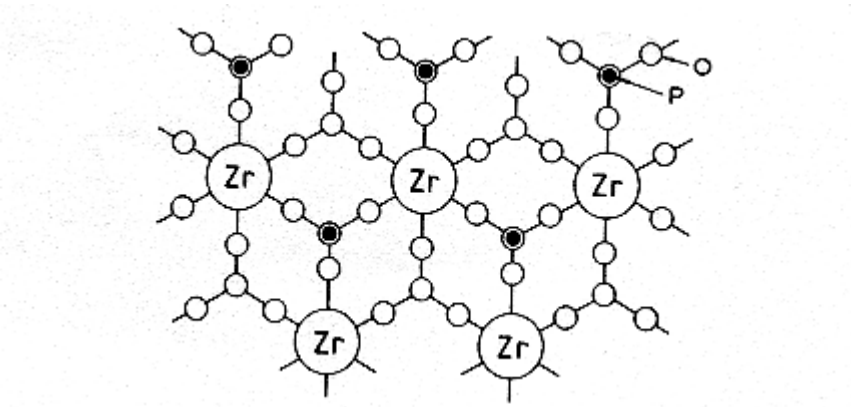

Figure 3.13 Structure of Zirconium Phosphate [42]

The first maximum in the XRD pattern of the crystalline polymers is generally assumed to be corresponding to the interlayer distance, which varies with the size and charge of the interlayer cations as given in Table 3.23 [42]. The interlayer distance for zirconium phosphate is 7.60 Å.

Table 3.23 The Interlayer Spacings (in Å) in Group IV Phosphates and Arsenates $M[H(P, As)O_4]_2.H_2O$

Group IV Element	Phosphates	Arsenates
Titanium	7.56	7.77
Zirconium	7.60	7.82
Tin	7.76	7.77
Cerium	10.95	9.10
Thorium	11.47	7.05

In our case, after filtering and drying , the first maximum in the XRD pattern of the product was around 7.5 Å. So, $Zr(HPO_4)_2.H_2O$ was formed firstly together with BPO_4. When this product was heated at 1100 ^oC, BPO_4 was still present but ZrP_2O_7 was also obtained. Then at 1200 ^oC, no BPO_4 lines were observed but only the lines of ZrP_2O_7 were present. This means that boron was entered to ZrP_2O_7 structure into interstitial positions, and the formula can be given as $ZrP_{2-x}B_xO_{7-x}$.

CHAPTER IV

CONCLUSIONS

In this work several phosphate and borophosphate compounds which contain BO_3, BO_4, and PO_4 complex anionic structures were investigated by **a)** solid state reaction, **b)** flux reactions, and **c)** hydrothermal method. The compounds were identified by XRD, IR, DTA and EDX methods.

In solid state reactions;

The systematic investigation of $M^{II}O.M^{IV}O_2.B_2O_3.P_2O_5$ (where $M^{IV}= Zr^{4+}$, Si^{4+}, and $M^{II}=Ca^{2+}$, Sr^{2+}) reactions with different compositions was carried out in this research.

$ZrSr[BPO_7]$ was prepared first time in this study together with $Sr_7Zr(PO_4)_6$ and BPO_4 given by the following equation:

$$2ZrO_2(s) + 2SrCO_3(s) + B_2O_3(s) + 2(NH_4)_2HPO_4(s) \rightarrow 2ZrO_2.2SrO.B_2O_3.P_2O_5(s) + 4NH_3(g) + 3H_2O(g) + 2CO_2(g)$$

The unit cell parameters of the new phase ($ZrSr[BPO_7]$) were found as a=11.85Å, b=12.99 Å, c=17.32 Å in orthorhombic system.

In the further study, it is planned to produce single crystal of the product using hydrothermal method with different acids and different pH values.

In this study, it was also proved that the $SiZr[BPO_7]$ compound could be obtained through solid state reactions with a structure resembling $SrZr[BPO_7]$. The unit cell parameters were a=8.9243 Å, b=13.1548 Å, and c=5.4036 Å in orthorhombic system. Since at 1100 ^oC, only α-$Sr_2P_2O_7$ was the main product, the formation of $Sr_{2-x}Si_xP_{2-y}B_yO_7$ additional solid solution is expected.

By using different acids at different pH values and applying flux method, single crystal of this compound are going to be prepared in future.

The synthesis of $Al_2[BPO_7]$ and $B_2[BPO_7]$ was unsuccesful in the experiments, instead $AlPO_4$ and BPO_4 were obtained, respectively.

In the hydrothermal reactions, $Zr(HPO_4)_2.H_2O$ was formed firstly together with BPO_4. Then at 1100 ^oC, BPO_4 was still present but ZrP_2O_7 was also obtained. At 1200 ^oC, boron was entered to ZrP_2O_7 structure by occupying interstitial positions, and the formula can be given as $ZrP_{2-x}B_xO_{7-x}$.

In the future study, $M_2^{3+}[BPO_7]$ (where M^{3+} is the rare earth elements) type borophosphates will be investigated.

REFERENCES

[1] Muetteries E.L., ‘‘The Chemistry of Boron and Its Compounds’’, John Wiley Publ., New York, 1967.

[2] Wells A.F., Structural Inorganic Chemistry, Oxford, Clarendon Press, 1975.

[3] Kızılyallı M., Güvensoy E., Borik Asitin Bozunma Mekanizması, Kim. 88, V. Kimya ve Kimya Müh. Semp. Hacettepe Üniv., Ankara 21-23 Eylül, 1988.

[4] Berger S. V., Acta Chem.Scand., 7, 611, 1953.

[5] Krogh-Moe J., Phys. And Chem. of Glass., 1, 26, 1960.

[6] Zachariasen W.H., Z.Krist., 88, 150, 1934.

[7] Zachariasen W.H., Acta Cryst., 7, 305, 1954.

[8] Berger S. V., Acta Chem.Scand., 4, 1054, 1950.

[9] Takeuchi Y., Acta Cryst., 5, 574, 1952.

[10] Tazaki H., J. Sci. Hiroshima Univ., A10, 55, 1940.

[11] Bor Madenleri, DPT-2123, OIK-327, Mart, 1988.

[12] Türkiye Bor Mineralleri Envanteri, MTA, no:162, Ankara, 1976.

[13] Helvacı C., ‘Geology, Minerology and Geochemistry of the Borate Deposits Associated Rocks at the Emet Valley, Turkey. Doctoral Dissertation, University of Nottingham, England, 1977.

[14] Helvacı C., Stamatakis M.G., Zagouroglou C., Kanaris J., Explor. Mining Geol., 2(2), 171-178, 1993.

[15] Garrett D.E., ‘‘Borates, Handbook of Deposits, Processing, and Use’’, London, Academic Press, 1998.

[16] Gagin L.V., Borates: Economic Geology and Production, Ch.18, pp. 267-268, Min. Eng., AIMMPE, New York, 1985.

[17] Shelley S., Chem. Eng., p.179, 1994.

[18] Oberhofer A.W., Benko J.J., Drozd J.C., Cleaner for Automotive Engine Cooling Systems, U.S. Patent 3, 959, 166, 1976.

[19] Rosenfelder W.J., Chemistry and Industry, 413-416, 1978.

[20] Kistler R.B., Helvacı C., Ind. Min. and Rocks, 6, 171-186, 1994.

[21] Xu G., Composition for Killing Oncomelania, Chinese Patent, CN1077589, 1990.

[22] Zambrano A.R., Ferroboron, U.S. Patent 4, 509, 976, 1985.

[23] Tarasevich B.P., Isaeva L.B., Kuznetsov E.V., Zhenzhurist I.A., Steklo Keram., 5, 17-19, 1990.

[24] Corbridge D.E.C., The Structural Chemistry of Phosphorous, Elsevier Publication, Amsterdam, 1974.

[25] Akishin P.A., Rambidi N.G., Ezhov Y.S., Zh. Neorgan. Khim., 5, 747, 1960.

[26] Averbuch M.T., and Durif A.P., Topics in Phosphate Chemistry, World Scientific Publication, London, 1996.

[27] Kızılyallı M., J. Inorg. Nucl. Chem., 1976, 38, 483-486

[28] Kızılyallı M., Journal of the Less-Common Metals, 127, 1987, 147-154.

[29] Trunov V. K., Oboznenko Y. V., Sirotinkin S. P., Tskhelashvilli N. B., Inorganic Materials, 27, 11, 1991, 2370-2374.

[30] Anisimova N. Y., Chudinova N. N., Trunov V. K., Inorganic Materials, 29, 1, 104-105, 1993.

[31] Trunov V. K., Oboznenko Y. V., Sirotinkin S. P., Tskhelashvilli N. B., Inorganic Materials, 27, 9, 1991, 1993-1994.

[32] Anisimova N. Y., Chudinova N. N., Trunov V. K., Inorganic Materials, 29, 1, 106-109, 1993.

[33] Kızılyallı M., Darras M., Journal of Solid State Chemistry, 107, 373-380, 1993.

[34] Hamady A., Zid M. F., Jouini E. T., Journal of Solid State Chemistry, 113, 120-124, 1994.

[35] Bensch W., Koy J., Zeitschrift für Kristallographie, 210, 1995, 445.

[36] Ledain S., Leclaire A., Borel M. M., Raveau B., Acta Cryst., 1996, C52, 1593-1594.

[37] Averbuch M.T., Guitel J.C., Acta Crystalogr., B33, 1613-1615, 1977.

[38] Lii K.H., Chen Y.B., Su C.C., Wang S.L., J. Solid State Chem., 82, 156-160, 1989.

[39] Notholt A.J.G., Phosphate Rock in the CENTO Region (Iran, Pakistan and Turkey), CENTO, Ankara, 1977.

[40] Uztetik A., ‘‘Synthesis and Structures of Some New Gadolinium Phosphates’’, Ph.D. Thesis, METU, Ankara, 1992.

[41] Mosner P., Kalendova A., Koudelka L., Dyes and Pigments,45, (2000), 29-34.

[42] Ray N.H., Inorganic Polymers, Academic Press, London, 1978.

[43] Kniep R., Engelhardt H., Hauf C., Chem. Mat., 10, (1998), 2930.

[44] Ramamoorthy P., and Rockett T.J., J.Amer.Ceram.Soc., 57, (1974), 501-502.

[45] Bauer H., Zeitschrift für Anorganishe und Allgemeine Chemie, 337, (1965), 183.

[46] Bauer H., Zeitschrift für Anorganishe und Allgemeine Chemie, 345, (1966), 225.

[47] Kniep R., Gozel G., Eisenmann B., Röhr C., Asbrand M., and Kızılyallı M., Angew.Chem.Int.Ed.Engl., 33(7), (1994) 749.

[48] Gözel G., ‘‘Preparation and Structural Investigation of Alkaline-Earth Borophosphates’’, Ph.D. Thesis, METU, Ankara, 1993.

[49] Baykal A., Kızılyallı M., Gozel G., Kniep R., Cry.Res.Technol., 35, (2000), 3, 247-254.

[50] Baykal A., Gözel G., Kızılyallı M., Toprak M., Kniep R., Turk. J. Chem., 24, 2000, 381-388.

[51] Shi Y., Liang J., Zhang H., Liu Q., Chen X., Yang J., Zhuang W., Rao G., Journal of Solid State Chemistry, 135, 43-51, 1998.

[52] Pushcharovsky D.Y., Gobetchia E.R., Pasero M., Merlino S., Dimitrova O.V., J. Alloys and Compounds, 339, (2002), 70-75.

[53] Pan S., Wu Y., Fu P., Zhang G., Wang G., Guan X., Chen C., J.Crystal Growth, 236, (2002), 613-616.

[54] Liebertz J., and Stähr S., Zeitschrift Kristallographie, 160, (1982) 135.

[55] Bluhm K., and Park C.H., Zeitschrift für Naturforschung, 52b, (1997), 102.

[56] Wang G., Wu Y., Fu P., Liang X., Xu Z., Chen C., Chem. Mater., 2002, 14, 2044-2047.

[57] Yılmaz A., Bu X., Kızılyallı M., Kniep R., Stucky G. D., Journal of Solid State Chemistry, 156, 2, 2001, 281-285.

[58] Hauf C., Yılmaz A., Kizilyalli M., Kniep R., Journal of Solid State Chemistry, 140, 154-156, 1998.

[59] Li Z., Wu Y., Fu P., Pan S., Lin Z., Chen C., Journal of Crystal Growth, 255, 119-122, 2003.

[60] Bontchev R.B., Sevov S.C., Inorg. Chem., 35, 6910-6911, 1996.

[61] Shi Y., Liang J., Zhang H., Yang J., Zhuang W., Rao G., Journal of Solid State Chemistry, 129, 45-52, 1997.

[62] Mi J. X., Zhao J. T., Mao S. Y., Huang Y. X., Engelhardt H., Kniep R., Z. Kristallogr., 215, 2000, 201-202.

[63] Kniep R., Schafer G., Engelhardt H., Boy I., Angew.Chem.Int.Ed., 1999, 38(24), 3642-3644.

[64] Kniep R., Will H.G., Boy I., Röhr K., Angew.Chem.Int.Ed.Engl.36, (1997), 9, 1013-1014.

[65] Baykal A., Kızılyallı M., KniepR., J. Material Science, 35, (2000), 4621-4626.

[66] Yilmaz A., Bu X., Kızılyallı M., Stucky G., Chem. Mater., 12, (2000), 3243-3245.

[67] Schäfer G., Borrmann H., Kniep R., Microporous and Mesoporous Materials, 41, (2000), 161-167.

[68] Boy I., Stowasser F., Schafer G., Kniep R., Chem. Eur. J., 7, 4, 834-839, 2001.

[69] Kritikos M., Wikstad E., Wallden K., Solid State Sciences, 3, 2001, 649-658.

[70] Huang Y.X., Schäfer G., Cabrera W.C., Cardoso R., Schenlle W., Zhao J.T., Kniep R., Chem. Mater., 13, (2001), 4348-4354.

[71] Schäfer G., Carrillo-Cabrera W., Schenelle W., Borrmann H., Kniep R., Z. Anorg. Allg. Chem., 628, (1), 289-294, 2002.

[72] Zhao Y., Zhu G., Liu W., Zou Y., Pang W., Chem. Commun., 1999, 2219-2220.

[73] Bontchev R.B., Do J., Jacobson A.J., Inorg. Chem., 39, 4179-4181, 2000.

[74] Boy I., Schafer G., Kniep R., Z. Anorg. Allg. Chem., 627, (2), 139-143, 2001.

[75] Boy I., Hauf C., Kniep R., Z. Naturforsch. B, 1998, 53, 5/6, 631-633.

[76] Do J., Bontchev R.P., Jacobson A.J., Inorg. Chem., 39, 4305-4310, 2000.

[77] Bontchev R.P., Jacobson A.J., Materials Research Bulletin, 1893, 1-9, 2002.

[78] Asnani M., Ramanan A., Vittal J. J., Inorganic Chemistry Communications, 6(2003), 589-592.

[79] Yang G. Y., Sevov S. C., Inorg. Chem. 2001, 40, 2214-2215.

[80] Dumas E., Chouvy C.D., Sevov S.C., J. Am., Chem., Soc., 124, 6, 908-909, 2002.

[81] Gupta P.K.S., Swikart G.H., Dimitrijevic R., Hossain M.B., Amer. Mineral., 76, (1991), 1400-1407.

[82] Moore P.B., Ghose S., Amer. Mineral., 56, (1971), 1527-1538.

[83] Koudelka L., Mosner P., Materials Letters, 42, 2000, 194-199.

[84] Koudelka L., Mosner P., Journal of Non-Crystalline Solids 293-295, 2001, 635-641.

[85] Sevov S.C., Angew.Chem.Int.Ed.Engl., 35(22), (1996), 2630.

[86] Zhou M., Li K., Shu D., Sun B. D., Wang J., Materials Science Engineering A, 346, 1-2, 116-121, 2002.

[87] Goetzman K., Karlheinz D., Hans-Dieter N., and Ralf G., Patent CA, C09K015,1996.

[88] Yılmaz A., Ph.D. Thesis, Middle East Technical University, Ankara, 2000.

[89] Krishna R. M., Andre J. J., Rao J. L., Antholine W. E., Materials Research Bulletin, 34, 10/11, 1521-1525.

[90] Courtney I. A., Dunlap R. A., Dahn J. R., Electrochimica Acta, 45, 1999, 51-58.

[91] Ali A.B., Taibi M., Aride J., Boukhari A., Fidancev E.A., Viana B., Aschehoug P., J.Alloys and Compounds 323-324, (2001), 673-677.

[92] Almeida A. F. L., Vasconcelos I. F., Thomazini D., Valente M. A., Sombra A. S. B., Physica B: Condensed Matter, 322, 3-4, 2002, 276-288.

[93] Su Q., Liang H., Hu T., Tao Y., Liu T., J.Alloys and Compounds, 344, (2002), 132-136.

[94] Nazabal V., Fargin E., Labrygere C., Flem G. L., Journal of Non-Crystalline Solids 270, 2000, 223-233.

[95] Rao T.V.R., Reddy R.R., Ahammed Y.N., Parandamaiah M., Hussain N.S., Buddhudu S., Purandar K., Infrared Physics and Technology, 41, (2000), 247-258.

[96] Ding S.J., Zhang D.W., Wang P.F., Wang J.T., Materials Chemistry and Physics, 68, (2001), 98-104.

[97] Liang H., Su Q., Tao Y., Hu T., Liu T., J.Alloys and Compounds, 334, (2002), 293-298.

[98] Ternane R., Adad M.T.C., Panczer G., Goutaudier C., Dujardin C., Boulon G., Ariguib N.K., Ayedi M.T., Solid State Sciences, 4, (2002), 53-59.

[99] Liang H., Su Q.,Lu S., Tao Y., Hu T.D., Liu T., Materials Research Bulletin 1888, (2002), 1-9.

[100] Almeida A. F. L., Thomazini D., Vasconcelos I. F., Valente M. A., Sombra A. S. B., International Journal of Inorganic Materials, 3, 2001, 829-838.

[101] Behm M., Irvine J. T. S., Electrochimica Acta, 47, 2002, 1727-1738.

[102] Dodd A. J., van Eck E. R. H., Chemical Physics Letters, 365, (2002), 313-319.

[103] Surana S.S.L., Sharma Y.K, Tandon S.P., Materials Sicence and Engineering, B83, (2001), 204-209.

[104] Sharma Y.K, Tandon S.P., Suran S.S.L., Materials Sicence and Engineering, B77, (2000), 167-171.

[105] Fanciulli M., Bonera E., Carollo E., Zanotti L., Microelectronic Engineering, 55, 2001, 65-71.

[106] Adamczyk A., Handke M., Journal of Molecular Structure, 596, 2001, 47-54.

[107] Li B., Yue Z., Zhou J., Gui Z., Li L., Materials Letters, 54, 2002, 25-29.

[108] Adamczyk A., Journal of Molecular Structure, 614, 2002, 127-132.

[109] Baykal A., ‘‘Synthesis and Characterization of Alkaline Earth and Rare Earth Borophosphate Compounds’’, Ph.D. Thesis, METU, Ankara, 1999.

[110] Acta Chimica Scandinavia 22, 1968 (1822-1832).

APPENDIX A

Table A. The X-ray Powder Diffraction Data of $SrBPO_5$ (J.C.P.D.S. Card. No: 18-1270)

I/I_o	d(Å)	hkl
20	4,480	102
80	3,430	110
6	3,060	112
100	2,966	200
100	2,957	104
5	2,718	202
10	2,416	114
10	2,272	006
40	2,242	210
40	2,239	204
50	2,129	212
6	1,977	300
6	1,900	302
10	1,894	116
60	1,873	214
2	1,804	206
10	1,713	220
10	1,711	304
2	1,662	222
6	1,645	310
6	1,639	108
6	1,600	312
6	1,596	216
10	1,531	224
10	1,526	118
10	1,482	400,314
10	1,478	208
2	1,450	402

APPENDIX B

Table B. The X-ray Powder Diffraction Data of ZrO_2 (J.C.P.D.S. Card. No: 37-1484)

I/I_o	**d(Å)**	**hkl**	**I/I_o**	**d(Å)**	**hkl**
3	5,0870	001	4	1,5924	-131
14	3,6980	110	3	1,5822	-222
10	3,6390	011	8	1,5459	131
100	3,1650	-100	7	1,5393	-203
68	2,8410	111	5	1,5095	311
21	2,6230	200	5	1,4960	-312
11	2,6060	020	8	1,4777	113
13	2,5400	002	1	1,4520	320
2	2,4990	-201	2	1,4486	230
4	2,3340	120	<1	1,4343	032
<1	2,2845	012	2	1,4262	-231
<1	2,2527	-211	6	1,4201	023
12	2,2138	-112	4	1,4165	-132
5	2,1919	201	1	1,3615	231
5	2,1805	-121	<1	1,3494	321
7	2,0203	211	<1	1,3398	-322
6	1,9910	-202	2	1,3253	-223
2	1,8593	-212	4	1,3217	-401
18	1,8481	220	1	1,3113	400
22	1,8187	022	1	1,3089	-232
13	1,8038	-221	<1	1,3035	040
5	1,7830	-122	<1	1,3005	312
11	1,6937	003	<1	1,2862	-313
<1	1,6772	221	2	1,2700	004
11	1,6571	310	4	1,2647	140
9	1,6524	-311	1	1,2455	-114
6	1,6439	031	<1	1,2321	330
7	1,6100	-113	<1	1,2230	401

APPENDIX C

Table C. The X-ray Powder Diffraction Data of $Sr_7Zr(PO_4)_6$ (J.C.P.D.S. Card. No: 34-65)

I/I_o	d(Å)	hkl
10	4,1410	211
12	3,5890	220
100	3,2110	310
40	2,7140	321
10	2,1640	332
16	2,0720	422
30	1,9910	431
3	1,8530	521
<1	1,7400	530
12	1,6464	532
6	1,6046	620
7	1,5660	541
2	1,4965	631
3	1,4651	444
<1	1,4074	640
5	1,3811	721
3	1,3562	642
1	1,3328	730
4	1,2889	732
1	1,2687	800
1	1,2130	653
2	1,1963	822
4	1,1798	750
2	1,1490	752
<1	1,1073	842
2	1,0945	761
<1	1,0819	664

APPENDIX D

Table D. The X-ray Powder Diffraction Data of α-$Sr_3(PO_4)_2$ (J.C.P.D.S. Card. No: 24-1008)

I/I_o	**d(Å)**	**hkl**
1	6.600	003
7	4.554	101
1	4.225	012
10	3.393	104
100	3.016	015
85	2.694	110
<1	2.494	113
<1	2.418	107
3	2.318	021
11	2.271	202
11	2.198	009
2	2.186	018
14	2.110	024
7	2.087	116
35	2.009	205
20	1.821	1010
2	1.799	027
2	1.757	211
<1	1.736	122
9	1.703	119
1	1.661	214
20	1.611	125
12	1.555	300
6	1.509	0210

APPENDIX E

Table E. The X-ray Powder Diffraction Data of α-$Sr_2P_2O_7$ (J.C.P.D.S. Card. No: 24-1011)

I/I_o	d(Å)	hkl	I/I_o	d(Å)	hkl	I/I_o	d(Å)	hkl
35	7.400	110	11	2.525	150	3	1.776	071
13	6.600	020	7	2.422	321	4	1.747	441
3	5.300	120	10	2.406	122	3	1.742	171
3	5.010	011	2	2.377	241	2	1.722	520
11	4.462	200	5	2.310	202	8	1.703	062
9	3.940	130	2	2.274	212	6	1.680	511
4	3.694	220	6	2.239	331	12	1.669	203
85	3.439	201	9	2.230	100	13	1.665	033
100	3.406	031	30	2.195	060	4	1.656	213
35	3.327	211	6	2.132	160	3	1.651	271
4	3.291	040	1	2.090	251	2	1.640	521
15	3.182	131	65	2.044	232	3	1.637	133
25	3.128	230	7	1.987	430	<1	1.618	223
2	3.087	140	8	1.982	161	3	1.601	432
7	3.048	221	9	1.976	312	7	1.590	370
20	2.900	310	11	1.966	421	4	1.564	460
45	2.700	002	2	1.913	322	3	1.555	143
25	2.680	141	6	1.891	242	3	1.530	313
2	2.648	240	17	1.866	431	2	1.525	371
14	2.554	311	30	1.850	261	3	1.503	461

APPENDIX F

Table F. The X-ray Powder Diffraction Data of BPO_4 (J.C.P.D.S. Card. No: 34-132)

I/I_o	**d(Å)**	**hkl**
100	3.6351	101
3	3.3207	002
4	3.0699	110
34	2.2546	112
2	1.9719	103
10	1.8641	211
5	1.8175	202
<1	1.6604	004
1	1.5354	220
10	1.4597	213
<1	1.4146	301
<1	1.3936	222
2	1.3732	310
5	1.3192	204
4	1.2689	312
2	1.2114	303
4	1.1851	321
1	1.1272	224
<1	1.1069	006
2	1.0964	215
<1	1.0859	400
1	1.0580	314, 323
3	1.0402	411
<1	1.0319	402
<1	0.9862	206
1	0.9781	332
<1	0.9511	413
<1	0.9319	422

APPENDIX D

Table D. The X-ray Powder Diffraction Data of $Sr_3(PO_4)_2$ (J.C.P.D.S. Card. No: 32-1251)

I/I_o	**d(Å)**
100	3,29
80	3,02
20	2,75
14	2,29
7	2,24
30	2,05
35	1,97
15	1,84
7	1,65

APPENDIX H

Table H. The X-ray Powder Diffraction Data of SiO_2 (J.C.P.D.S. Card. No:15-26)

I/I_o	**d(Å)**	**hkl**
100	2.959	110
18	2.246	101
1	2.090	201
35	1.981	111
14	1.870	210
50	1.530	211
18	1.478	220
10	1.333	002
4	1.322	310
2	1.291	221
25	1.235	301
10	1.215	112

APPENDIX I

Table I. The X-ray Powder Diffraction Data of α-$CaZr(PO_4)_2$ (J.C.P.D.S. Card. No:30-293)

I/I_o	**d(Å)**
100	9.82
20	8.05
60	4.99
100	4.59
60	4.42
100	4.11
60	3.93
60	3.63
60	3.44
70	3.29
60	3.05

APPENDIX J

Table J. The X-ray Powder Diffraction Data of $CaZr(BO_3)_2$ (J.C.P.D.S. Card. No:24-349)

I/I_o	d(Å)	I/I_o	d(Å)
80	3.700	60	1.584
40	3.250	60	1.495
20	3.020	20	1.466
100	2.920	20	1.441
60	2.470	40	1.426
20	2.300	20	1.381
60	2.220	40	1.343
40	2.070	20	1.323
60	2.020	40	1.265
20	1.890	20	1.243
100	1.823	40	1.181
20	1.668	40	1.142
40	1.604		

APPENDIX K

Table K. The X-ray Powder Diffraction Data of $CaZr_4(PO_4)_6$ (J.C.P.D.S. Card. No:33-321)

I/I_o	d(Å)	hkl	I/I_o	d(Å)	hkl
3	7.5560	003	8	1.9483	0210
4	7.2080	101	2	1.9134	315
22	6.3160	012	32	1.8989	226
69	4.5460	104	2	1.8895	0012
82	4.3920	110	5	1.8760	042
6	3.8960	015	1	1.8130	2011
100	3.7980	113	1	1.8033	404
1	3.6070	202	23	1.7807	2110
63	3.1594	024	5	1.7679	137
3	2.9140	205	1	1.7538	045
95	2.8651	116	1	1.7358	1112
5	2.6559	018	2	1.7004	1013
26	2.5643	214	12	1.6924	318
44	2.5355	300	2	1.6759	1211
3	2.4286	125	16	1.6679	324
2	2.4040	303	28	1.6597	410
8	2.2735	208	2	1.6286	235
6	2.1965	220	2	1.6212	413
7	2.1860	119	7	1.5840	0114
4	2.1734	1010	7	1.5793	048
4	2.1507	217	15	1.5446	1310
12	2.1062	306	2	1.5366	327
2	2.0745	312	16	1.5197	416
25	2.0191	128	1	1.5159	3012
15	1.9777	134	11	1.4904	2014

APPENDIX L

Table L. The X-ray Powder Diffraction Data of α-$CaZr(PO_4)_2$ (J.C.P.D.S. Card. No:33-320)

I/I_o	d(Å)	hkl	I/I_o	d(Å)	hkl
50	7.870	001	20	1.968	004
50	4.496	110	10	1.929	222
35	4.265	-200	30	1.823	-204, -114
20	3.953	111	18	1.783	114
100	3.930	002	5	1.750	204
7	3.848	111, -201	4	1.732	-223
9	3.663	201	3	1.727	130
90	3.005	-112	3	1.660	420
20	2.975	-202	4	1.623	510
70	2.917	112	8	1.588	-132
20	2.814	202	12	1.585	-314
16	2.646	020	12	1.578	024
5	2.623	003	12	1.575	132
20	2.503	021, 310	6	1.554	-422
4	2.292	-113, -203	3	1.529	-512
5	2.248	220	10	1.511	314
3	2.237	113	10	1.506	422
20	2.195	022	12	1.503	-205, -224
10	2.160	-312	10	1.499	-115, 330
4	2.131	400	2	1.473	512
10	2.067	312	2	1.472	115
16	1.977	-222	5	1.459	224

APPENDIX M

Table M. The X-ray Powder Diffraction Data of $AlPO_4$ (J.C.P.D.S. Card. No:11-500)

I/I_o	d(Å)	hkl	I/I_o	d(Å)	hkl
1	5.010	110	3	1.5823	042
100	4.077	111	3	1.5452	421
3	3.553	020	5	1.5074	332
3	3.539	200	3	1.4431	422
3	3.496	002	3	1.4341	224
10	3.162	021, 201	1	1.4101	403
10	2.867	112	3	1.3789	134
20	2.506	220	1	1.3630	511
5	2.491	202, 022	1	1.3582	333
5	2.135	311, 131	3	1.3474	115
3	2.038	222	3	1.3104	423
7	1.949	203, 023	3	1.2913	512
5	1.888	312, 132	<1	1.2443	044, 404
<1	1.779	040	1	1.2333	441
3	1.770	400	1	1.2151	530
3	1.749	004	<1	1.1977	531
3	1.7072	223	1	1.1936	513
1	1.6510	114	1	1.1866	315
5	1.6250	331	<1	1.1794	442
3	1.6163	133			

APPENDIX N

Table N. The X-ray Powder Diffraction Data of $Al_5(BO_3)O_6$ (J.C.P.D.S. Card. No:34-1039)

I/I_o	**d(Å)**	**hkl**	**I/I_o**	**d(Å)**	**hkl**
1	7.500	020	1	1.939	171
100	5.378	021	1	1.874	310
30	4.374	111	15	1.845	153
13	3.850	002	10	1.821	311
10	3.754	040	1	1.787	063
70	3.376	041	5	1.777	172
15	3.197		13	1.710	134
1	2.840	200	20	1.686	262
80	2.690	042	10	1.590	204
20	2.508	151	10	1.566	191
8	2.429	023	1	1.530	281
8	2.309	113	30	1.514	263
10	2.259	240	5	1.475	352
20	2.186	152	2	1.465	244
45	2.113	133	10	1.449	282
1	2.002	170	5	1.417	400
8	1.949	242			

APPENDIX O

Table O. The X-ray Powder Diffraction Data of H_3BO_3 (J.C.P.D.S. Card. No:30-199)

I/I_o	**d(Å)**	**hkl**
80	6.020	101
10	5.460	011
10	3.500	102
10	3.380	012
100	3.190	112
20	2.900	221
5	2.810	212
80	2.670	030
5	2.573	130
5	2.504	031
20	2.300	113
40	2.248	231
20	2.206	-
5	2.075	421
20	2.025	412
20	1.862	044
20	1.706	233
20	1.673	-
5	1.612	-
10	1.597	333

APPENDIX P

Table P. The X-ray Powder Diffraction Data of $Na_2Zr(PO_4)_6$ (J.C.P.D.S. Card. No:35-125)

I/I_o	d(Å)
85	7.280
10	4.969
25	4.068
70	3.904
11	3.867
8	3.739
7	3.364
17	3.028
5	2.936
100	2.889
5	2.840
70	2.637
30	1.939
25	1.937
10	1.845
5	1.722

APPENDIX R

Table R. The X-ray Powder Diffraction Data of $Na_{5-4x}Zr_{1+x}(PO_4)_3$ (J.C.P.D.S. Card. No:37-384)

I/I_o	d(Å)
75	7.284
10	6.012
20	4.921
35	4.567
10	4.419
30	4.029
65	3.893
10	3.861
5	3.734
10	3.344
10	3.019
25	2.977
15	2.948
30	2.909
100	2.887
10	2.695
75	2.633
10	2.516
20	2.179
15	2.155

APPENDIX S

Table S. The X-ray Powder Diffraction Data of ZrP_2O_7 (J.C.P.D.S. Card. No:24-1490)

I/I_o	d(Å)	hkl	I/I_o	d(Å)	hkl
30	4.76	333	4	1.9993	1230
100	4.12	600	3	1.9449	1233
30	3.68	630	9	1.8922	993
25	3.368	633	15	1.8433	1260
1	3.222	731	2	1.8003	1263
1	3.134	732	2	1.7748	1350
1	3.052	811	10	1.6833	1266
1	2.984	821	2	1.6460	1290
25	2.917	660	2	1.6363	1293
2	2.747	090	13	1.5872	999
1	2.715	911	1	1.5622	1551
1	2.615	930	3	1.5317	1506
30	2.489	933	3	1.5056	1563
6	2.378	666	10	1.4576	12120
4	2.288	906	1	1.4339	1730
-	2.213	1120	2	1.4138	1590
2	2.205	963	9	1.3917	1593
2	2.163	1131	9	1.3745	1800
1	2.093	1062	1	1.3557	1830
3	2.061	1200	3	1.3372	1833

APPENDIX T

Table T. The X-ray Powder Diffraction Data of $H_2ZrP_2O_8$ (J.C.P.D.S. Card. No:21-395)

I/I_o	d(Å)
100	7.37
20	4.98
80	4.48
60	3.93
80	3.53
20	3.21
40	2.91
80	2.50
20	2.35
20	2.24
40	2.13
40	2.04
60	1.85
20	1.79
40	1.73
40	1.68
40	1.66
10	1.59
60	1.53
60	1.33
60	1.32
40	1.28
40	1.25

APPENDIX U

Table T. The X-ray Powder Diffraction Data of α-$Zr(HPO_4)_2$ (J.C.P.D.S. Card. No:31-1486)

I/I_o	**d(Å)**	**hkl**
100	7.41	002
40	4.59	-111
45	4.28	-112
13	4.12	111
100	3.75	-113
20	3.54	-204
20	3.22	202
12	3.12	211
25	2.75	212
30	2.67	020
40	2.63	021
6	2.52	022
5	2.48	121
4	2.40	204
4	2.35	311
10	2.28	-107
9	2.26	016
25	2.13	400
6	2.09	-117
7	2.05	-406
8	2.00	-321
30	1.87	321